AD-A102 705 CASE WESTERN RESERVE UNIV CLEVELAND OH CASE LABS FOR--ETC F/G 20/1
COMPUTER CONTROLLED RESONATOR MEASUREMENTS WITH A 12-LITER PYRE--ETC(U)
JUN 81 M A BARRETT-GUELTEPE, M E GULTEPE N00014-75-C-0557
UNCLASSIFIED TR-48 NL

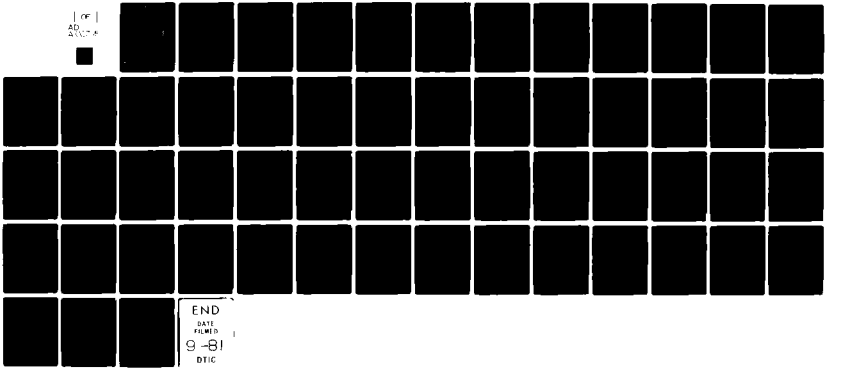

END
DATE FILMED
9-81
DTIC

LEVEL II

12

OFFICE OF NAVAL RESEARCH

Contract N00014-75-C-0557
Project NR 384-305

TECHNICAL REPORT NO. 48

COMPUTER CONTROLLED RESONATOR MEASUREMENTS WITH A 12-LITER PYREX SPHERE AND A 100-LITER TITANIUM SPHERE.

by

M.A. Barrett-Gültepe, M.E. Gültepe and E.B. Yeager

Ultrasonic Research Laboratory
and
Case Laboratories for Electrochemical Studies
Case Institute of Technology
Case Western Reserve University
Cleveland, Ohio 44106

(11) 30 June 1981

Unclassified

SECURITY CLASSIFICATION OF THIS PAGE (When Data Entered)

REPORT DOCUMENTATION PAGE		READ INSTRUCTIONS BEFORE COMPLETING FORM
1. REPORT NUMBER: 48 ✓	2. GOVT ACCESSION NO.: AD-A102	3. RECIPIENT'S CATALOG NUMBER: 705
4. TITLE (and Subtitle): COMPUTER CONTROLLED RESONATOR MEASUREMENTS WITH A 12-LITER PYREX SPHERE AND A 100-LITER TITANIUM SPHERE		5. TYPE OF REPORT & PERIOD COVERED: Technical Report
		6. PERFORMING ORG. REPORT NUMBER
7. AUTHOR(s): M.A. Barrett-Gültepe, M.E. Gültepe and E. B. Yeager		8. CONTRACT OR GRANT NUMBER(s): N00014-75-C-0557
9. PERFORMING ORGANIZATION NAME AND ADDRESS: Ultrasonic Research Laboratory, Case Western Reserve University, Cleveland, Ohio 44106		10. PROGRAM ELEMENT, PROJECT, TASK AREA & WORK UNIT NUMBERS: NR384-305
11. CONTROLLING OFFICE NAME AND ADDRESS: Office of Naval Research, Physics Section -Code 421, Arlington, VA 22217		12. REPORT DATE: 30 June 1981
		13. NUMBER OF PAGES: 50
14. MONITORING AGENCY NAME & ADDRESS(if different from Controlling Office)		15. SECURITY CLASS. (of this report): Unclassified
		15a. DECLASSIFICATION/DOWNGRADING SCHEDULE

16. DISTRIBUTION STATEMENT (of this Report)

Approved for public release; distribution unlimited

17. DISTRIBUTION STATEMENT (of the abstract entered in Block 20, if different from Report)

18. SUPPLEMENTARY NOTES

19. KEY WORDS (Continue on reverse side if necessary and identify by block number)

acoustic spherical resonator, ultrasonic absorption, ultrasonic relaxation, computer techniques

20. ABSTRACT (Continue on reverse side if necessary and identify by block number)

A microcomputer controlled spherical resonator apparatus has been developed for acoustic studies of liquids at 5-500 kHz. A programmable frequency synthesizer producing frequencies in steps down to 1μHz is used as the source. The received signal is fed into a programmable tuned amplifier, and demodulated. A/D conversion is made with a high-speed sample-and-hold digital voltmeter via a multiplexing scanner. The system allows for very detailed mode mapping of the sphere by accumulating amplitude data both while the sphere is being driven and after a specified decay time interval, along with recording of temperature.

DD FORM 1 JAN 73 1473 EDITION OF 1 NOV 65 IS OBSOLETE

S/N 0102-LF-014-6601

Unclassified

SECURITY CLASSIFICATION OF THIS PAGE (When Data Entered)

over

Continued (Block #20)

The experimental resonance frequencies have been compared with those predicted theoretically and decay rates of a large number of resonances measured. The amplitude decay can be followed through 70 dB with reproducibility within ± 0.2 dB/s under favorable conditions. The system is also used for cylindrical resonators.

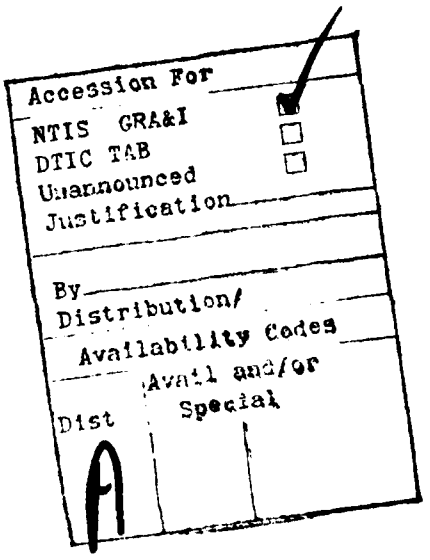

TABLE OF CONTENTS

LIST OF FIGURES

LIST OF TABLES

I. Introduction

Measurements of absorption and velocity of sound in liquids in the lower MHz and KHz region involves some difficulties. If one extends the limits of the pulse-echo technique down to such frequencies, very long acoustical paths and large quantities of samples are necessary making these measurements impractical.

By means of acoustic resonators it is possible to increase the effective path length through multiple reflections enabling measurements of absorption and velocity while keeping sample volumes and container sizes minimum. Two types of resonators are most commonly used; cylindrical and spherical. Cylindrical resonators are most useful for velocity measurements because the dimensions of the cylinder can be controlled and measured precisely.

In a spherical resonator, the resonance frequencies of radial modes are approximate integer multiples of frequencies having the wavelength twice the diameter of the sphere, with a correction for the vessel walls. Radial modes are of greatest interest because of the minimum shear and consequently minimum energy loss at the wall. In cylindrical shaped resonators, two types of resonance modes are of interest: radial modes and the axial mode. In the radial mode the cylinder cross section perpendicular to the axis, circumferentially expands and contracts. In contrast to radial modes in both cylinder and spheres, the axial mode is influenced by the height of the liquid filling the cylinder. The Q values (or the sharpness of the resonance of a resonator) of the cylinders are very much lower than those of the spheres. This influences the way they are used.

The attenuation coefficient of the liquid encapsulated in a resonator can be measured in the following three ways: 1) measuring the rate of decay of the stored acoustic energy in a resonator. The rate of decay of the resonator filled with fluid is proportional to the attenuation in the medium and the attenuation due to the imperfect reflection at the resonator walls.

2) By measuring the sharpness of the resonator and using the relation between Q and the absorption coefficient $Q = \frac{\omega \times \text{energy stored in resonator}}{\text{energy decay rate in resonator}}$ where ω is the angular frequency.

3) In cylindrical resonators, by measuring the standing wave ratio and relating this to absorption coefficient.

II. Previous experimental techniques

The first systematic work on the resonator technique was made by Leonard[1] and Wilson[2]. They used various 12 and 50 liter spherical pyrex vessels for resonators. The principle of their resonator technique involves the storage of the acoustic energy in a resonator by exciting the vessel by means of a driver (generally a piezoelectric transducer) and the measurement of decay rate of the stored energy after the driver is turned off. In their experiment the driving transducer was used as a receiver after the transducer was separated from the driving electronic circuit by means of a relay. The decaying acoustic signal was amplified and received. The decay rate (logarithm of the decaying amplitude against time) was measured with a sound level recorder.

Up to the present, the above basic spherical resonator technique of Leonard has been used with a few minor improvements, namely:

1) Two transducers were used instead of a single one

2) Recently frequency synthesizers have been substituted for the signal generators where high stability is required.

3) It has been reported[3] that by making a reservoir pump system part of a spherical resonator, chemicals can be added without disturbing the vessel.

In a recent abstract[4] measurements are described on the velocity of sound in gases with an accuracy of 10ppm with a spherical resonator. No details of the experimental technique are given.

In the case of cylindrical resonators, somewhat similar progress has been made since the systematic study of Lambert[5]. Various devices or configurations have been utilized for velocity and absorption measurements in the frequency range of 100 Hz[6] to as high as 36 MHz[7]. Both axial and radial modes of propagation of sound in cylindrical cavities were used for absorption and velocity measurements in the various studies described in the literature. Labhardt and Schwarz[7] have described a low volume cylindrical cavity resonator for measurements of the absorption and the speed of sound in liquids. Their manual measurements on velocity of sound in water after correction for wall losses gave results with ±20 ppm reproducibility in the frequency range of 400 KHz to 36 MHz.

Anderson and Hampton[6] measured the speed of sound in water with an impedence tube by means of a so called "automatic impedance computer" (possibily a transfer function analyzer). The value they obtained for sound speed in water at 20°C is $\sim$ 20% less than the established value in the literature. They attributed this difference to the compliance of the tube walls.

Shumway[8] has used a cylindrical plastic resonator for measuring absorption and velocity of sound in sediments. Using the lower radial modes of this resonator, he obtained fairly good agreement between his measurements for water around 25 KHz and high frequency measurements obtained with interferometers.

III. Limitations of the previous manual experimental techniques and the justification of the computer controlled experiments

As we mentioned earlier, in addition to the imperfect reflection of sound waves from resonator walls and their contributions to the measured losses, there are other difficulties which are inherent to large resonators i.e. particularly spherical resonators can make measurements difficult and results less meaningful:

1) A so-called "mode mapping" of a spherical resonator must be made to establish the resonance frequencies of the particular resonator under study. Although it is in theory possible to calculate the frequencies of the radial modes of a sphere if the radius and wall thickness are known, all investigators using spherical resonators have found in practice that the frequencies showing the lowest decay rates do not fall at regularly spaced intervals, contrary to the theory for a perfect sphere. Therefore, to find all the frequencies of value for absorption measurements requires a search over the entire frequency range. Because of the very high Q values, the peaks can only be detected with a search in steps of the order of a Hz. This is only practical with a computer. Further, it is well known that the radial modes do not show decay rates smoothly varying with frequency, and the accepted practice is to consider those with the slowest decay rates as the most reliable for indicating absorption

in the sample. Thus comparison must be made between the promising modes before selecting the less lossey radial modes for the proposed study.

2) As the speed of sound changes, the resonance frequency of the resonator changes. This is commonly encountered when the chemical constituents are added into the resonators. The search must then be repeated to locate the new resonance frequencies. This is a very time consuming process even with a synthesizer used as a signal source. Changes in temperature produce a similar problem.

3) In the cylindrical and spherical resonators, a particular resonance peak for a certain mode may appear assymmetrical and exhibit shoulders. This is due to coupling of one or more different modes to the one under study. Measurments on such frequencies should be avoided. Manual examination of such peaks on the oscilloscope while sweeping the frequency is a time consuming process and judgment is a subjective one.

4) Although in the ideal situation radial modes are equally spaced throughout the working frequency range of the vessel, at the higher frequencies there are an increasing number of other modes, and separation of the radial modes from these becomes tedious. To overcome these difficulties, statistical reverberation has generally been used in which a decay of a band of frequencies is followed. The assumption is made that as time increases the decay rate observed becomes that of the slowest decaying radial modes. However, in these frequencies the difference between decay rates of the radial and other modes becomes small and therefore separation becomes

impractical. The measured decay rate is likely to be a combination of several modes, and therefore prone to error.

It is clear from the above discussion that the difficulties make the method labor intensive, and therefore well suited to automatic control by a computer. In this way, mapping can be carried out in fine steps, utilizing the entire 24 hours of the day, except for limitations imposed by other factors such as temperature instability. It is therefore also possible to extend the range in which individual frequencies are studied instead of going over to statistical reverberation.

IV. Description of the Computer Controlled Resonator

A. Data processing system

The data processing system consists of a dedicated microcomputer, its peripheral devices and some input-output devices. The schematic diagram of the data processing system, along with the mechanical apparatus is given in Fig. 1.

1. The dedicated microcomputer

The dedicated microcomputer is a 6502 microprocessor based 8-bit computer, Commodore 2001-32 furnished with IEEE-488 bus, GPIB (General purpose interface bus) with 32K memory. This computer is capable of handling BASIC of binary code machine language. In order to input the readings from a i/o device with a maximum speed using the IEEE-488 bus, it is necessary to use machine language rather the BASIC's "input" and "print" statements. With our microcomputer, the fastest data transfer rate as character string is approximately 75 readings sec^{-1} in 8-byte ASCII* format, with

*ASCII-American Standard Code for Information Interchange

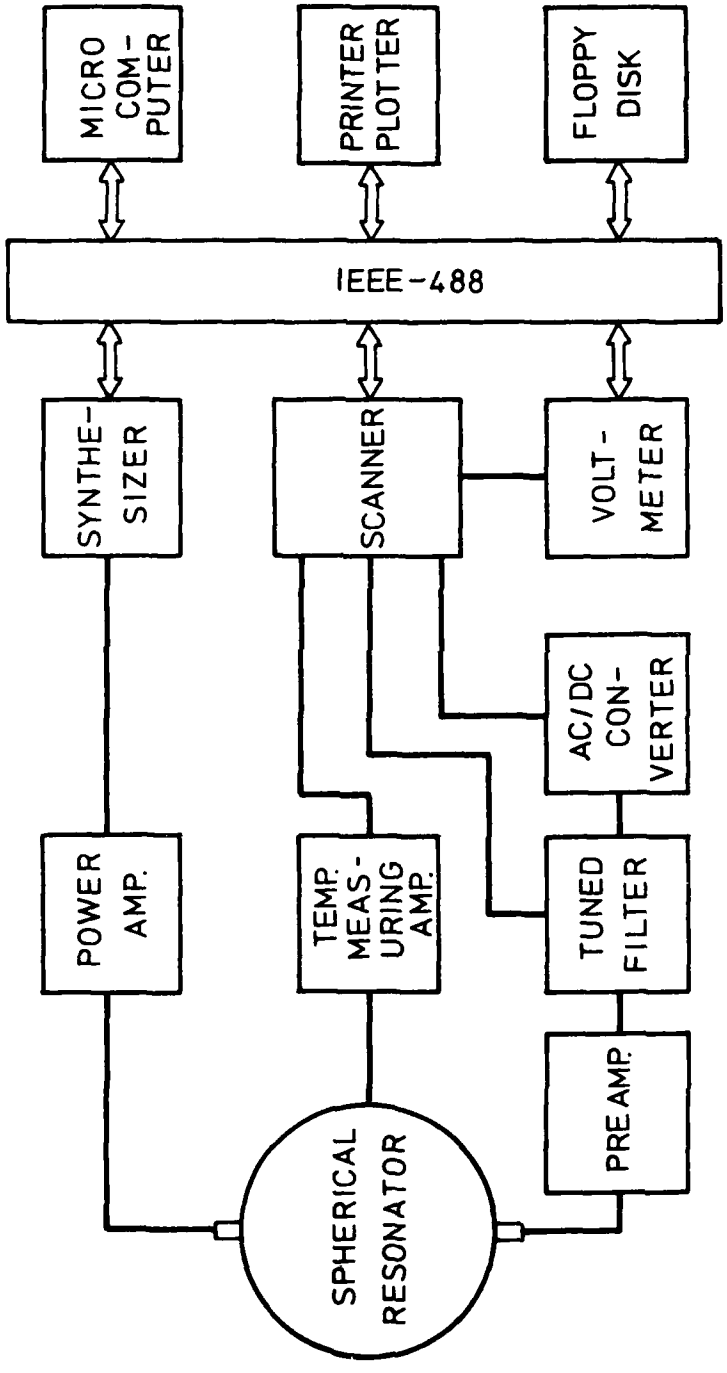

Fig. 1. Block diagram of the computer controlled resonator apparatus.

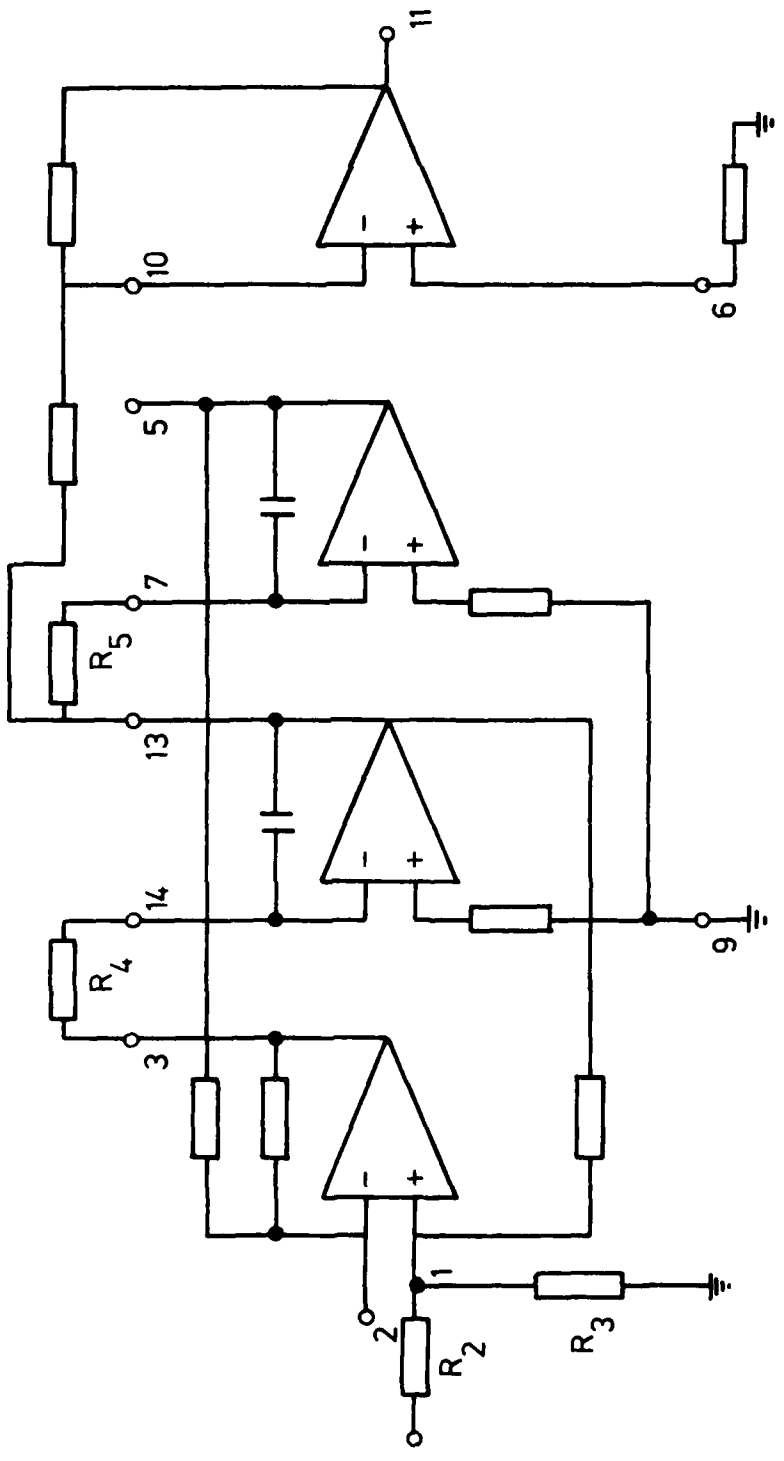

Fig. 2. Block diagram of the computer tuned band pass filter and amplifier.

BASIC, and 2500 readings sec^{-1} in 2-byte PACKED format using machine language (the voltmeter is triggered from the users port, making use of one of the 6522 timers).

2. Synthesizer/function generator

The synthesizer (Hewlett-Packard Model 3325A) is a fully programmable signal generator through the GPIB. The synthesizer can produce sine waves at a minimum frequency of 1 μHz and a maximum frequency of 20 MHz. The frequency may be selected with up to eleven digits of resolution. In the frequency range employed in this work, 5 kHz-400 kHz, at a given frequency this instrument produces a sine wave with harmonic distortion relative to the fundamental no greater than -60 dB.

3. Power Amplifier

The output of the synthesizer is fed to a broad band power amplifier which is capable of producing 3 Watts maximum output of 600 Ω optimum load.

4. Receiving amplifier and computer tuned band pass filter

In the early stages of this work, output from the receiving crystal was fed to a cathode follower input stage of a model RBL-5 radio receiver (National Company Inc.). This receiver is manually tunable in the frequency range of 15 kHz to 500 kHz. Before every 8-24 hrs. run, the receiver was tuned to cover a range 2-10 kHz wide, the greater width being possible at the higher frequencies.

An alternative arrangement allowing for full automation is to feed the signal from the receiving crystal to the Hewlett-Packard Model 465A wide band amplifier and impedance converter (10MΩ-50Ω). This

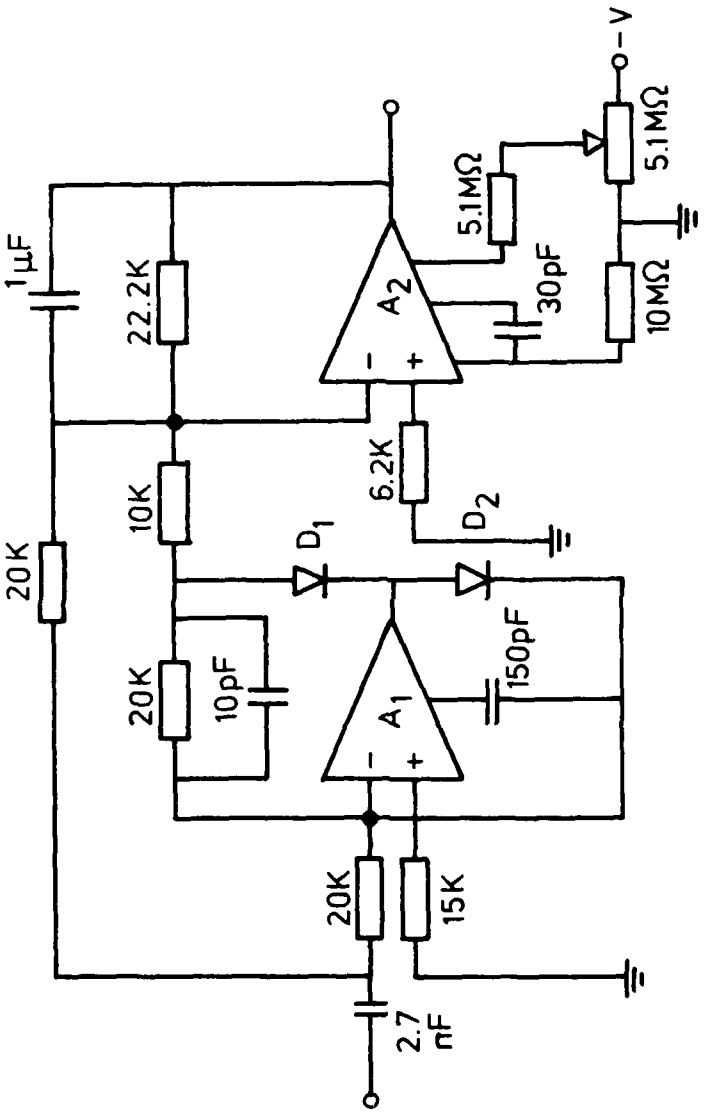

Fig. 3. Block diagram of the AC/DC converter. A_1 and A_2 are LM 101 H; D1 and D2 are FD700.

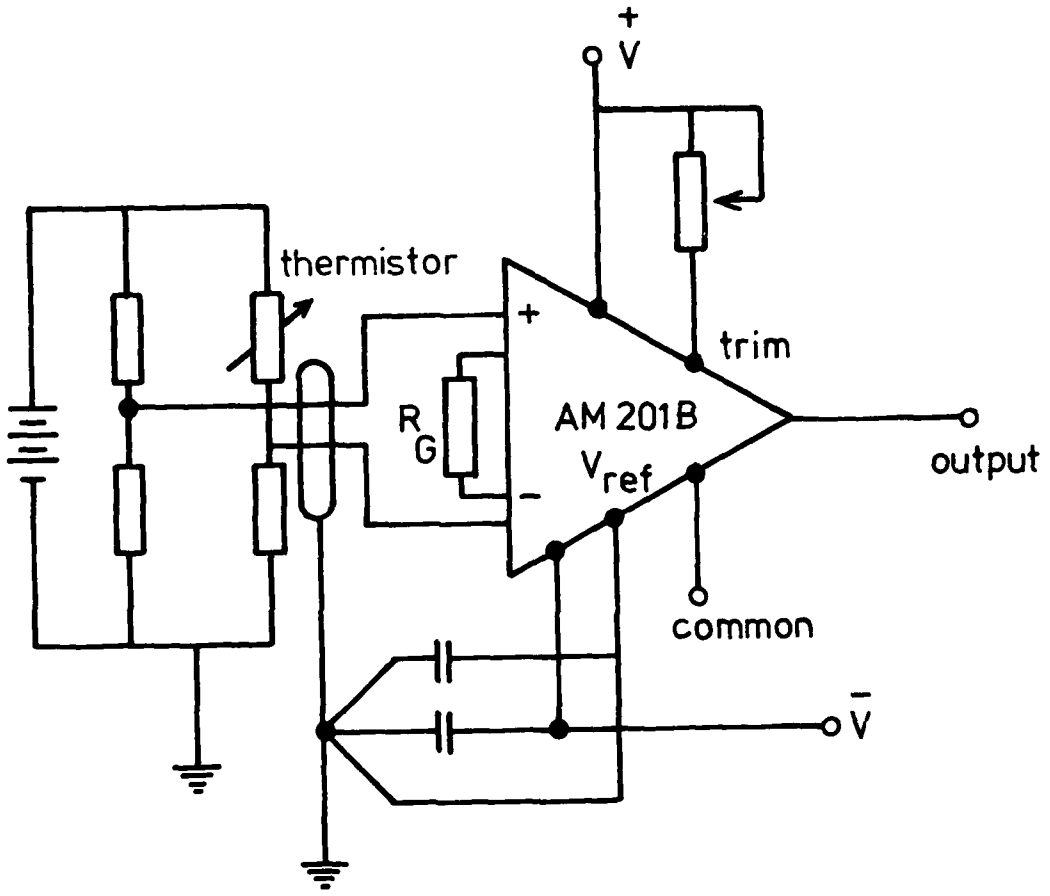

Fig. 4. Temperature measuring circuit.

amplifier has selectable gain of 20 dB or 40 dB over a continuous frequency range of 5 Hz to 1 MHz. Because of the high input impedance of the amplifier, no impedance matching between crystal and the amplifier is needed.

After amplification, the signal is fed to an active filter, Model FLT-U2 Datel Systems Inc., Mansfield, MA. The schematic diagram of the FLT-U2 wired up as an adjustable Q, band pass filter is given in fig. 2. Frequency tuning is adjusted by two external resistors, and Q tuning by a third external resistor. In order to maintain constant bandwidth and vary the center frequency, R_4 is kept constant and R_5 is varied with the aid of the scanner's actuator relay plug-in card (see below for further description of the scanner). The tuned signal is then fed into the built-in amplifier for final amplification.

5. AC/DC Converter

The exponentialy decaying amplitude of the tuned signal is fed to an AC/DC converter to obtain its envelope. The schematic diagram of the AC/DC converter* is given in fig. 3. This is essentially a full wave rectifier with averaging filter and is useful up to 500 kHz. The converter was adjusted to be linear over 80 dB.

6. Temperature measurements

A calibrated thermistor which forms one arm of a resistance bridge is located very near the neck of the spherical resonator. The millivolt level output of the bridge is amplified by an instrumentation

*This circuit is basically the one given in "linear application handbook", National Semiconductor 1978, with a few modifications.

amplifier before being fed into one of the channels of the low thermal relay plug-in card of the scanner. The instrumentation amplifier used has low overall voltage offset drift characteristics and introduced insignificant error in temperature measurements over a long time period. The schematic diagram of the measuring circuit is given in fig. 4.

7. Scanner

The scanner (Hewlett-Packard, Model 3495A) is a fully programmable multi-switch. The scanner may listen on the GPIB, but is not capable of talking to the controller (microcomputer). This instrument is also furnished with high speed (1 msec) scanning capability. In our experiment the scanner has been used in the following manner.

The outputs of the AC/DC converter and the temperature measuring instrumentation amplifier is fed into a low thermal relay plug-in card, for one input per channel. The low thermal relay card is 20-to-1 multiplexer, allowing 20 different signals (DC voltages) to be monitored by one voltmeter (see below), one at a time.

As mentioned above, the active filter FLT-U2 is tuned to a working frequency with the desired Q by means of switching various resistors into the circuit. For this purpose the appropriate resistors were connected to the terminals of the actuator relay plug-in card. The relays have two sets of normally open contacts with four terminals per channel. Unlike low thermal relays, any number of these relays may be closed and opened simultaneously as needed.

8. Digital Voltmeter

The multiplexed output of the low thermal relay card is fed into a high speed sample-and-hold digital voltmeter (model 3437A system voltmeter, Hewlett-Packard). The output data is sent to

the microcomputer via the GPIB in ASCII (8-byte) format. The voltmeter is capable of sampling voltages at rates up to 5700 samples per second, which is somewhat faster than the controller is capable of receiving the data.

9. Periferals

A digital printer-plotter (Hewlett-Packard Model 7245A) is used to plot the results and print the processed data. A 350K byte dual floppy disk, Commodore 2040, is used to store programs and data.

B. Apparatus

A 12 liter, round bottom pyrex boiling flask was used as the spherical resonator for the major part of the work described in this report. The neck of the flask has been reduced in size by glass blowing to a 3" long and 1/2" diameter cylindrical shape. From this access point, the resonator is filled, emptied and degassed. By measuring the volume of the liquid required to form a smooth continuation of the curvature of the sphere at the neck of the flask, and the circumference of the flask, the following constants of the vessel were calculated. The weight of the empty vessel provided a check on the figure for the wall thickness:

outside diameter = 29.33 cm

average wall thickness = .304 cm

The resonator is placed over a triangle formed by stretching piano wire inside a ring. Three 5" long bars welded into this ring form feet in tripod fashion. The tension of these piano wires is sufficient that point contacts are established between the sphere and the wires. The sphere and the supporting ring is placed on a plate which forms the bottom of a bell jar.

The electrical connections (transducer and thermistor leads) were made with various feed-through connectors attached to the base plate. The bell jar and base plate are thermostated with circulating thermostating liquid in closely spaced copper tubes which line the inside of the bell jar and the top face of the bottom plate. Over the bell jar 2" thick cast polyurethane forms a thermal blanket. The bell jar is evacuated with a rotary vacuum pump. With suitable supports, two ceramic crystals are used for driving the resonator and monitoring the decay amplitude.

In addition to the 12 l glass resonator, a 100 l titanium sphere is also used. This sphere is on loan from Office of Naval Research, and is one of the boyancy tanks of the deep diving research submarine ALVIN. Apart from a very smooth equatorial weld, a 2" flat portion at the bottom and a small opening at the top, the sphere is claimed to have uniform sphericity to one thousandth of an inch.

A similar construction is used to suspend this sphere to that mentioned above with the exception that stainless steel multicore aircraft cables are used in place of piano wire. The cables are stretched to attain the smallest possible area of contact with the sphere.

At the north pole of the sphere, an inlet/outlet assembly is attached. This is made entirely of titanium and stainless steel, and is capable of operating up to 6000 psi (the titanium sphere is authorized for use up to 4500 psi). At the present time the assembly is used to fill, empty, or circulate the contents at reduced or atmospheric pressure, with the aid of an all stainless steel and teflon circulation pump.

All wetted parts of this system are made out of corrosion resistant materials, ie. 316 stainless steel, titanium and teflon.

C. Preparation of the resonators for experiment

It was found that complete degassing of the 12 l resonator is achieved after subjecting the liquid in the sphere to high-powered (100 Watts) ultrasonic waves under vacuum for about 24 hrs. After this lengthy ultrasonic treatment around a $0.2^{o}C$ temperature gradient is established between the top and bottom of the sphere. The liquid must be mixed thoroughly before placing the resonator in the bell jar. Crystals are coupled to the sphere with light grease. Pressure is applied until the maximum received signal is observed.

Degassing the 100 l titanium sphere presents an interesting challange. While it was possible to remove the 12 l sphere for degassing, this is clearly not practicle with the 100 l sphere. A 10" diameter hole cut into the base plate enables attaching a nickel stack which is driven by a Raytheon 10 kHz magnetostrictive driver oscillator. The already existing four screw holes on the south pole of the sphere is used for attaching the nickel stack. Considerably longer degassing time is needed for the 100 l sphere than the 12 l sphere.

V. Experimental Results

A. Mode mapping the 12 liter resonator

In order to establish the resonance frequencies of the sphere, a search was made in the following manner, using the program described in flow chart I. In a given frequency range, generally 1 kHz at a time, a total of 1500 frequency points were taken. This corresponds

FLOW CHART I

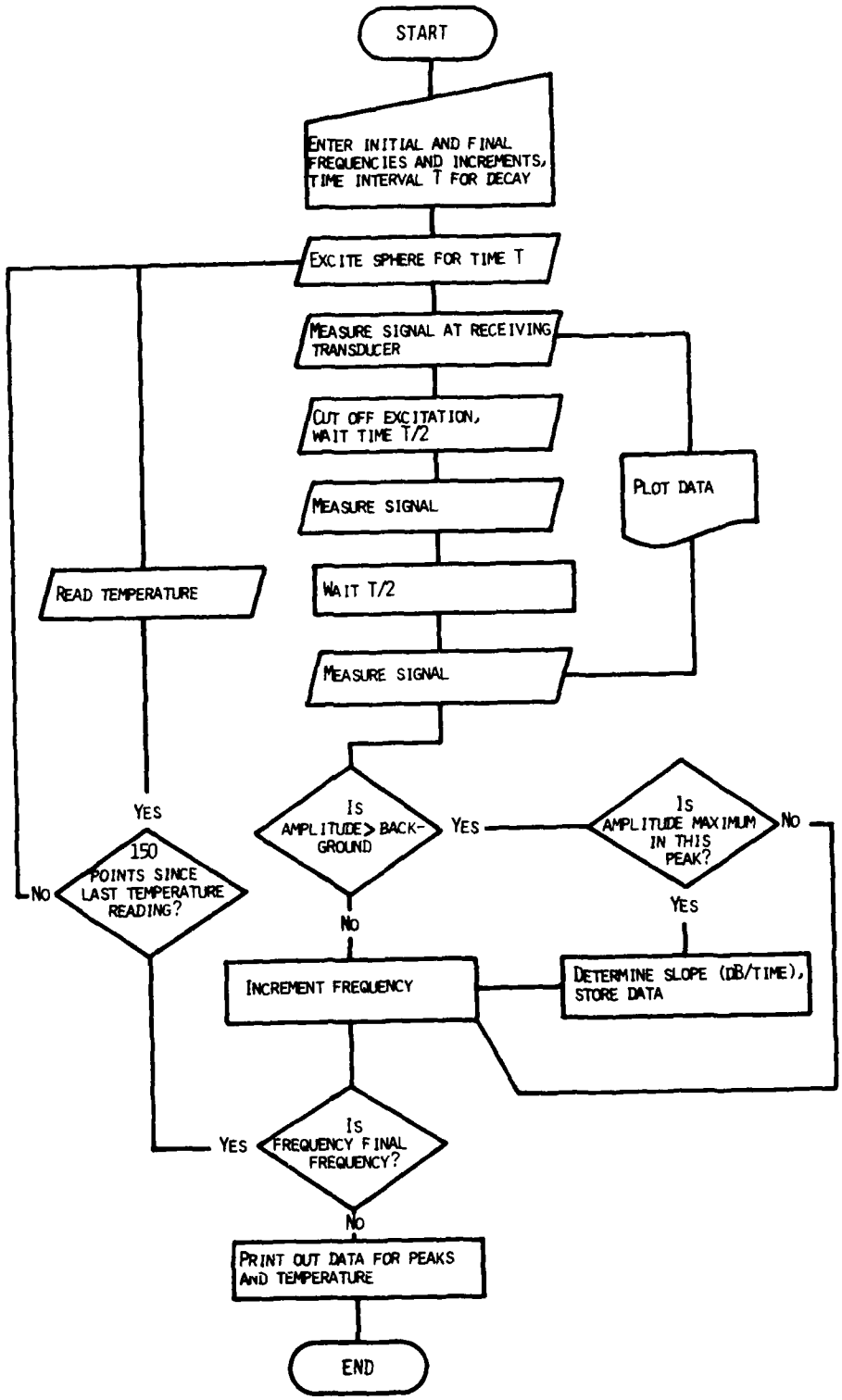
START
ENTER INITIAL AND FINAL FREQUENCIES AND INCREMENTS, TIME INTERVAL T FOR DECAY
EXCITE SPHERE FOR TIME T
MEASURE SIGNAL AT RECEIVING TRANSDUCER
CUT OFF EXCITATION, WAIT TIME T/2
MEASURE SIGNAL
WAIT T/2
MEASURE SIGNAL
PLOT DATA
READ TEMPERATURE
Is AMPLITUDE > BACK-GROUND
Yes
Is AMPLITUDE MAXIMUM IN THIS PEAK?
No
Yes
No
150 POINTS SINCE LAST TEMPERATURE READING?
Yes
No
INCREMENT FREQUENCY
DETERMINE SLOPE (DB/TIME), STORE DATA
Is FREQUENCY FINAL FREQUENCY?
Yes
No
PRINT OUT DATA FOR PEAKS AND TEMPERATURE
END

to 0.66 Hz steps. The sphere was first excited for a period of time which depended on the frequency: it takes longer to establish the steady state sound level in the ranges below 80 kHz than at higher frequencies. The amplitude during excitation was measured, and then the sound field was cut off. Two readings were taken during the chosen decay period. The amplitude taken at the end of the excitation period and at the end of the decay period were plotted as sound level in dB vs. frequency. Using the two readings taken during the decay period, a rough estimate was made of the decay slope for frequencies representing peaks. These approximate slopes were printed out after the scan was finished. These generally gave a good indication of the decay rate, but gave misleading results when there was excessive ringing. Fig. 5 illustrates the printer/plotter output. The top curve shown is the amplitude during excitation, and the bottom, the amplitude after the chosen decay period. Figs. 6 and 7 show the same range with shorter decay times. A comparison of three figures demonstrates how less structure is evident as the decay period is increased from 2 s to 3½ s. It is generally assumed that the early dying modes are not the radial modes. However, there are complications putting the identification of the radial modes in doubt.

At high frequencies modes are more crowded together, and decay rates much faster. Fig. 8 gives an example around 300 kHz.

B. Mode mapping the 100 liter sphere

Basically the same procedure was employed for mode mapping the 100 l sphere. However, because the peaks are extremely narrow even at low frequencies, the frequency steps must be much smaller. In addition

decay times are considerably longer. As a result, the mode mapping over a given frequency range is much more prolonged. For this reason, some steps have been taken in the mode mapping procedure to make it more efficient. First, the frequency steps were decreased on the first indication of the proximity of a peak. Second, the mode mapping program was combined with that for measuring decay rate, described in the next section, and the data referring to peaks transferred to disk for examination at a later time. These improvements save considerable time. Fig. 9 illustrates the mode mapping plot for 21-22 kHz, and a detailed section in the 22.7 kHz region is shown in Fig. 10.

C. Determination of decay rates

The frequencies showing promise of the scans were investigated more thoroughly, with the signal amplitude during the decay period being measured at the approximate rate of 18 readings/s, using the program outlined in flow chart II. These readings were plotted immediately as dB vs. time. Although the main part of the procedure was computer controlled, the portion of the curve to be used for a linear regression was chosen by the operater after each plot, to avoid portions with excess ringing, or any other irregularity. From the slopes, values for α/f^2 were calculated. The lowest of these are collected in table I and Fig. 11.

At the frequencies giving useful vales of α/f^2, the curve was generally linear through 50 dB, and sometimes up to 70 dB (the voltmeter and ac/dc converter were determined to be linear through this entire range). In general, frequencies near but not on the peak frequency showed some

TABLE I

Calculated radial modes, and experimentally found slowest decay modes for the 12-liter sphere filled with water. Frequencies in parentheses are shown because of good agreement with calculated frequencies although not giving the lowest decay rates.

m	Freq., kHz (theoret.)	Freq., kHz (experimental)	α/f^2 $s^2cm^{-1}x10^{17}$	m	Freq., kHz (theoret.)	Freq., kHz (experimental)	α/f^2 $s^2cm^{-1}x10^{17}$
1	4.962			27	138.51	139.98	52
2	9.935			28	143.71		
						147.26	42
3	14.927	14.811		29	148.91	(148.22)	82
						153.64	34
4	19.943			30	154.11	(154.23	68
		22.51	2096				
5	24.983			31	159.31	(159.51)	51
		28.33	2126				
6	30.046	30.042	1525	32	164.51	(164.49)	81
		32.20	960			169.15	46
7	35.13	34.08	733	33	169.71	(169.53)	
		37.79	716				
8	40.23	39.90	624	34	174.91	174.87	37
		42.10	517				
9	45.35	45.06	500	35	180.11		
		47.38	216				
10	50.48	50.61	215	36	185.32	(185.27)	
11	55.62	55.84	191	37	190.52		
		58.50	160				
12	60.77	60.79	151	38	195.73	(195.47)	
13	65.93	(65.72)	163	39	200.93	(200.53)	
		68.83	95				
14	71.09	71.40	145	40	206.13	(206.02)	
15	76.26	75.71	84	41	211.34	211.61	38
		79.10	60				
16	81.43	(81.50)	86	42	216.55		
		83.41	73				
17	86.61	(86.84)	147	43	221.75		
18	91.79	(91.76)	123	44	226.96		
						228.99	38
19	96.97	97.87	64	45	232.16		
		(100.48)	54				
20	102.16	(102.34)	96	46	237.37	(237.38)	
21	107.35			47	242.58		
						243.24	34
22	112.54	(112.51)	89	48	247.78		
		113.80	46			249.40	35
23	117.73			49	252.99	(252.85)	
24	122.92	123.17	46	50	258.20		
		124.21	41				
25	128.12			51	263.40		
26	133.31			52	268.61	268.46	34

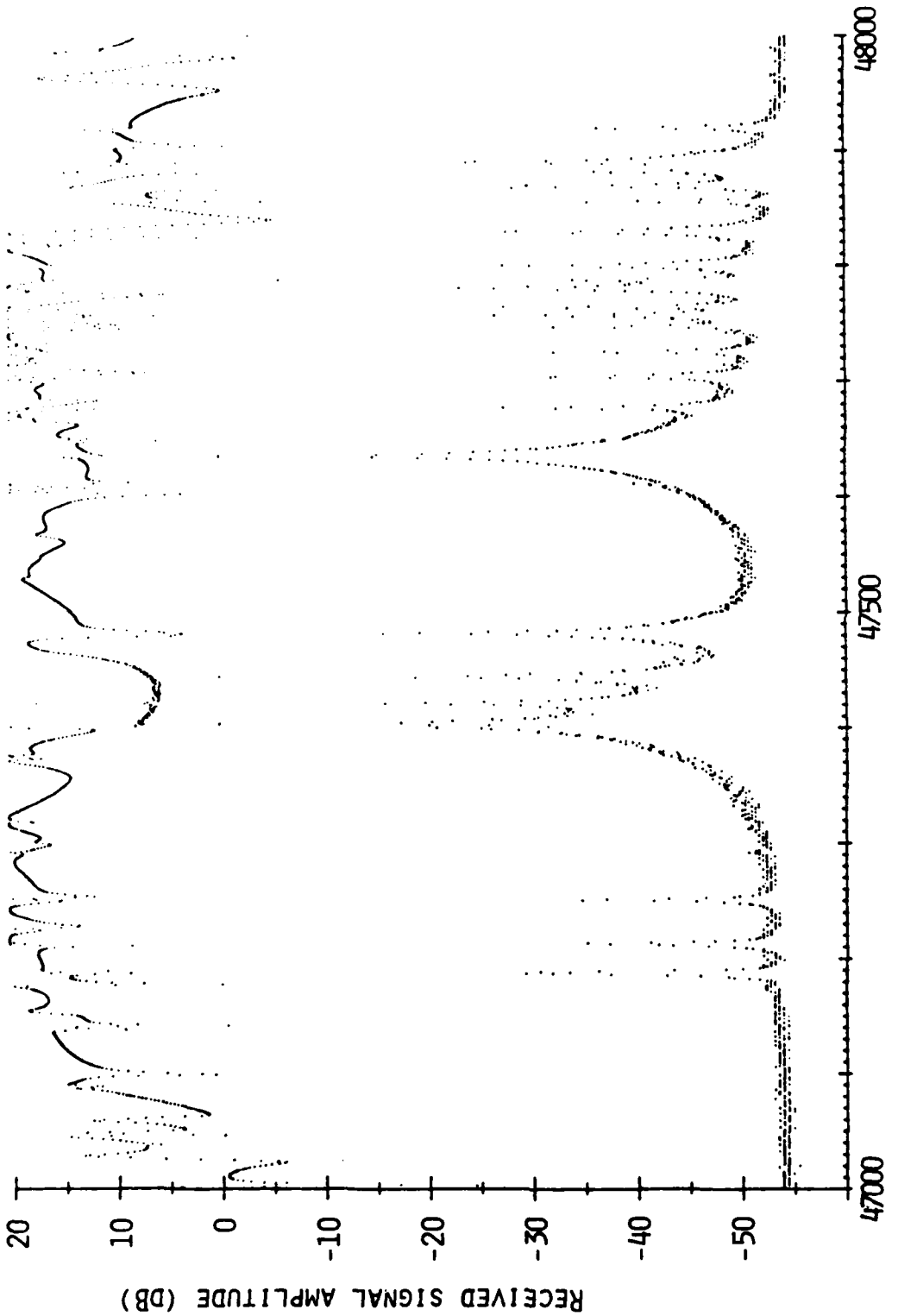

Fig. 5. Typical mode mapping plot of decay amplitude (dB) versus frequency for the 12-liter sphere filled with water. The lower curve was plotted after 2s delay, while the top curve was plotted during excitation. The total number of readings was 1500.

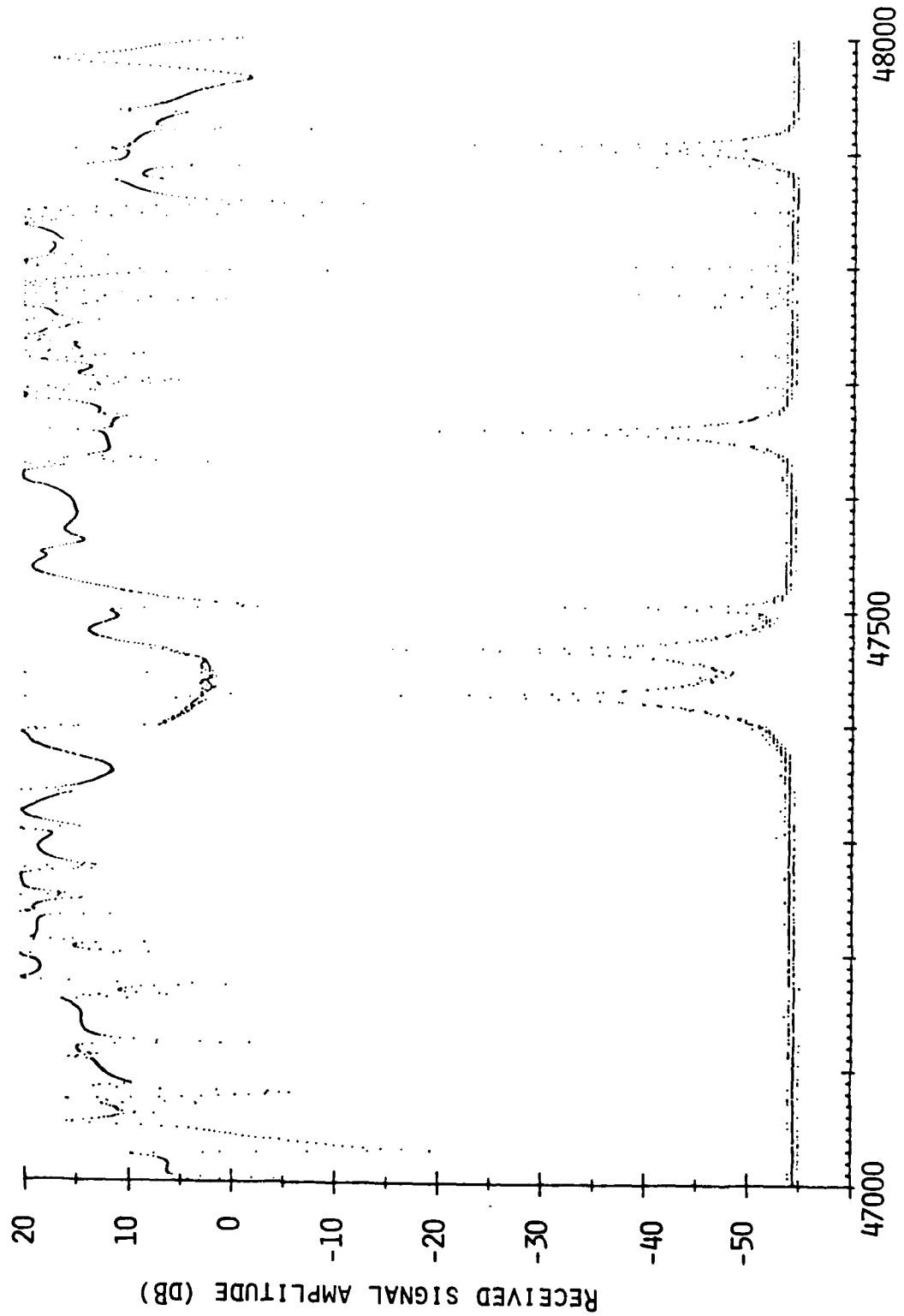

Fig. 6. As Fig. 5 but with 3s delay.

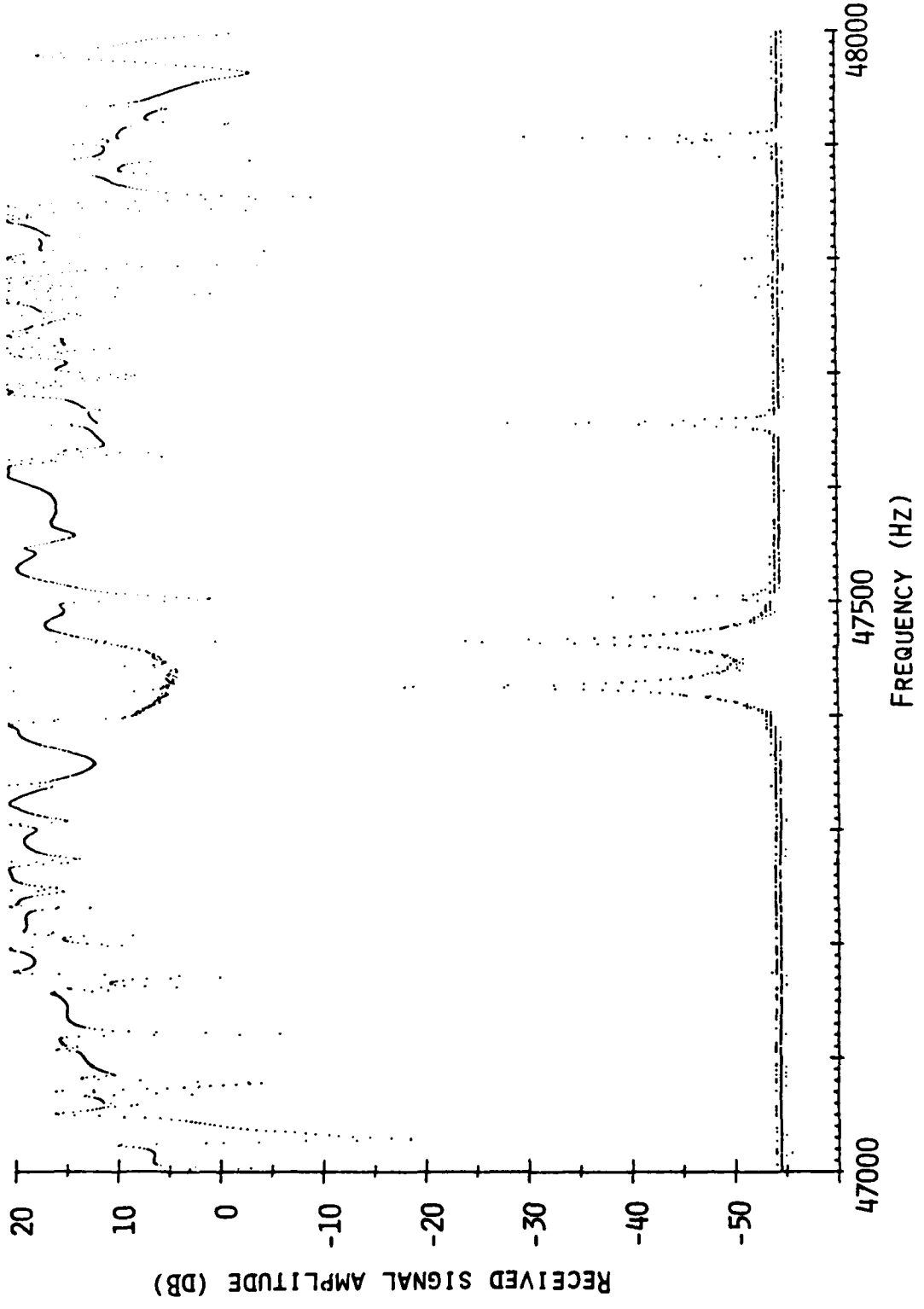

Fig. 7. As Fig. 5 but with 3¼s delay.

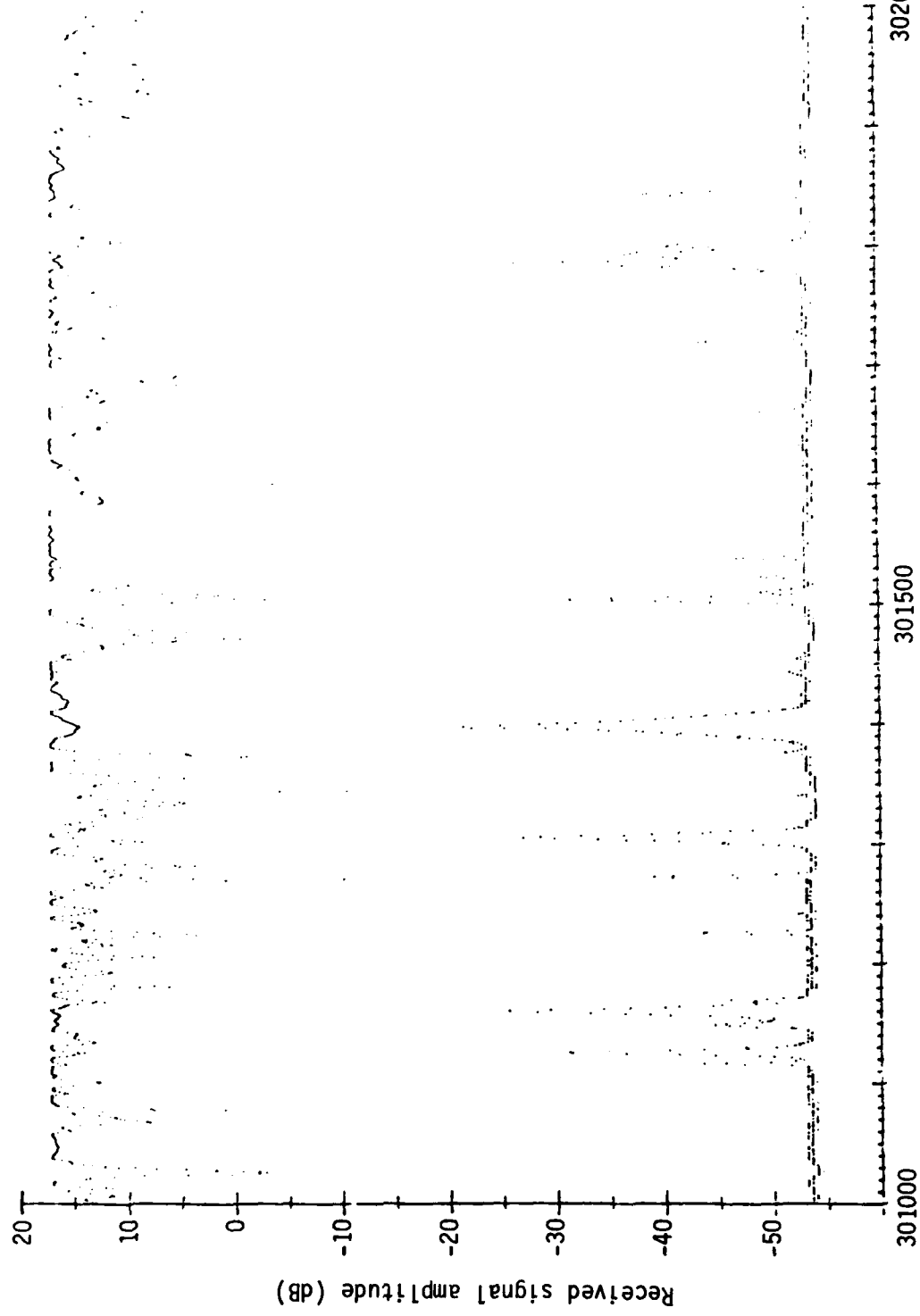

Fig. 8. Typical mode mapping plot of decay amplitude (dB) versus frequency for high frequencies using the 12-liter sphere filled with water. The lower curve was plotted after 0.5s delay. Total number of readings was 1500.

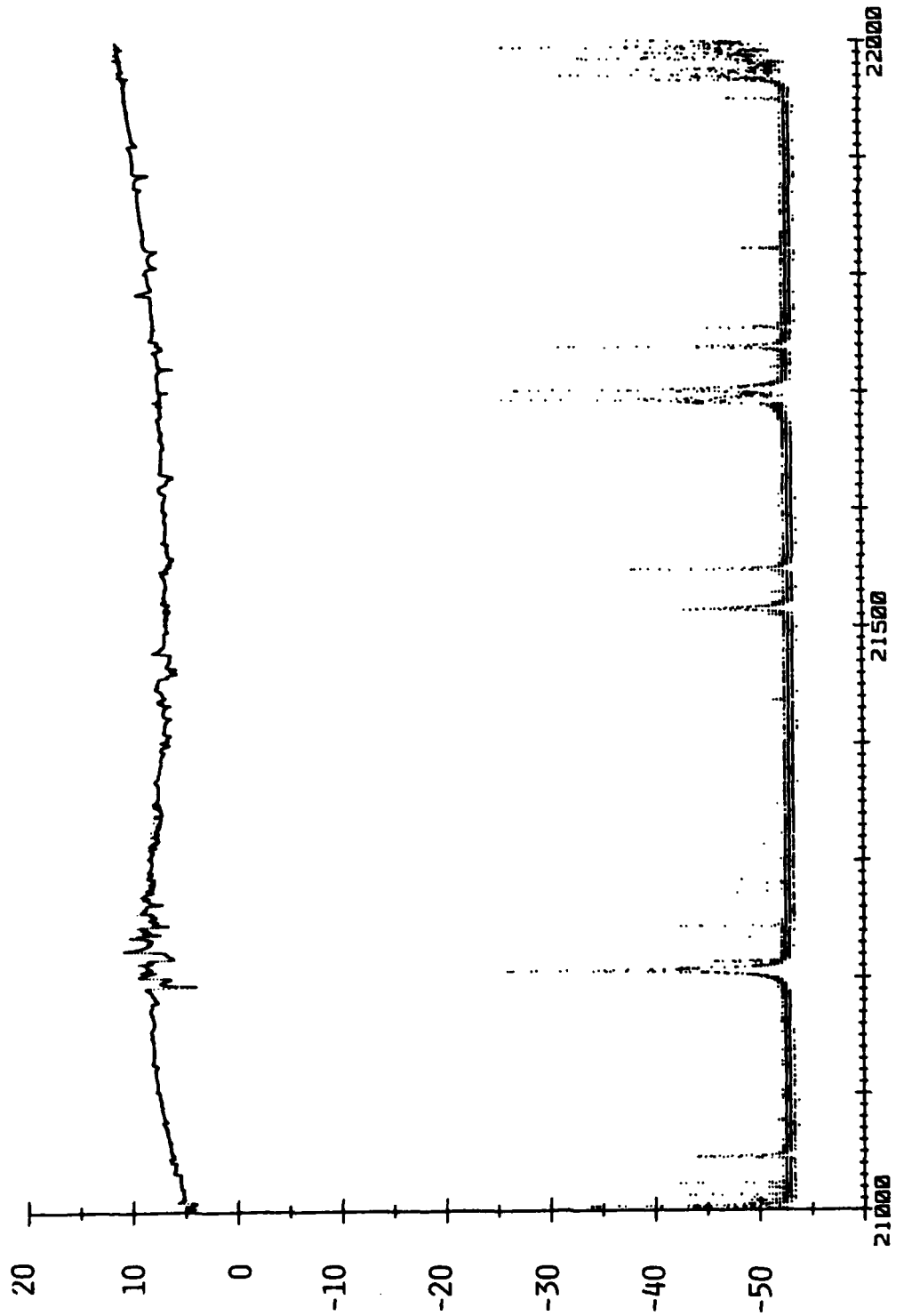

Fig. 9. Typical mode mapping plot of decay amplitude (dB) versus frequency using the 100-liter titanium sphere filled with water. The lower curve was plotted after 2s delay. The total number of readings was 20,000.

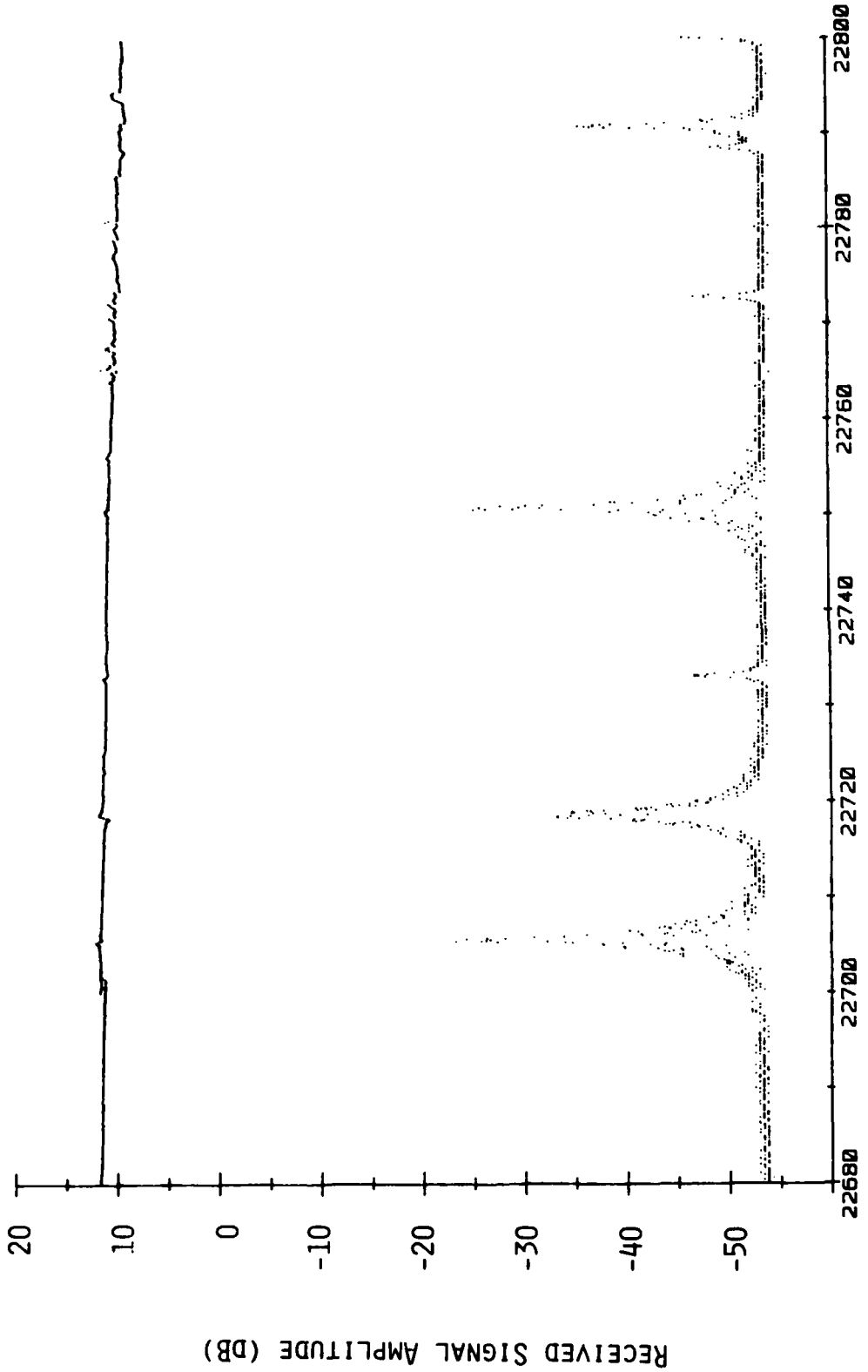

Fig. 10. Detailed mode mapping of decay amplitude (dB) versus frequency around 22.7 kHz using the 100-liter titanium sphere filled with water.

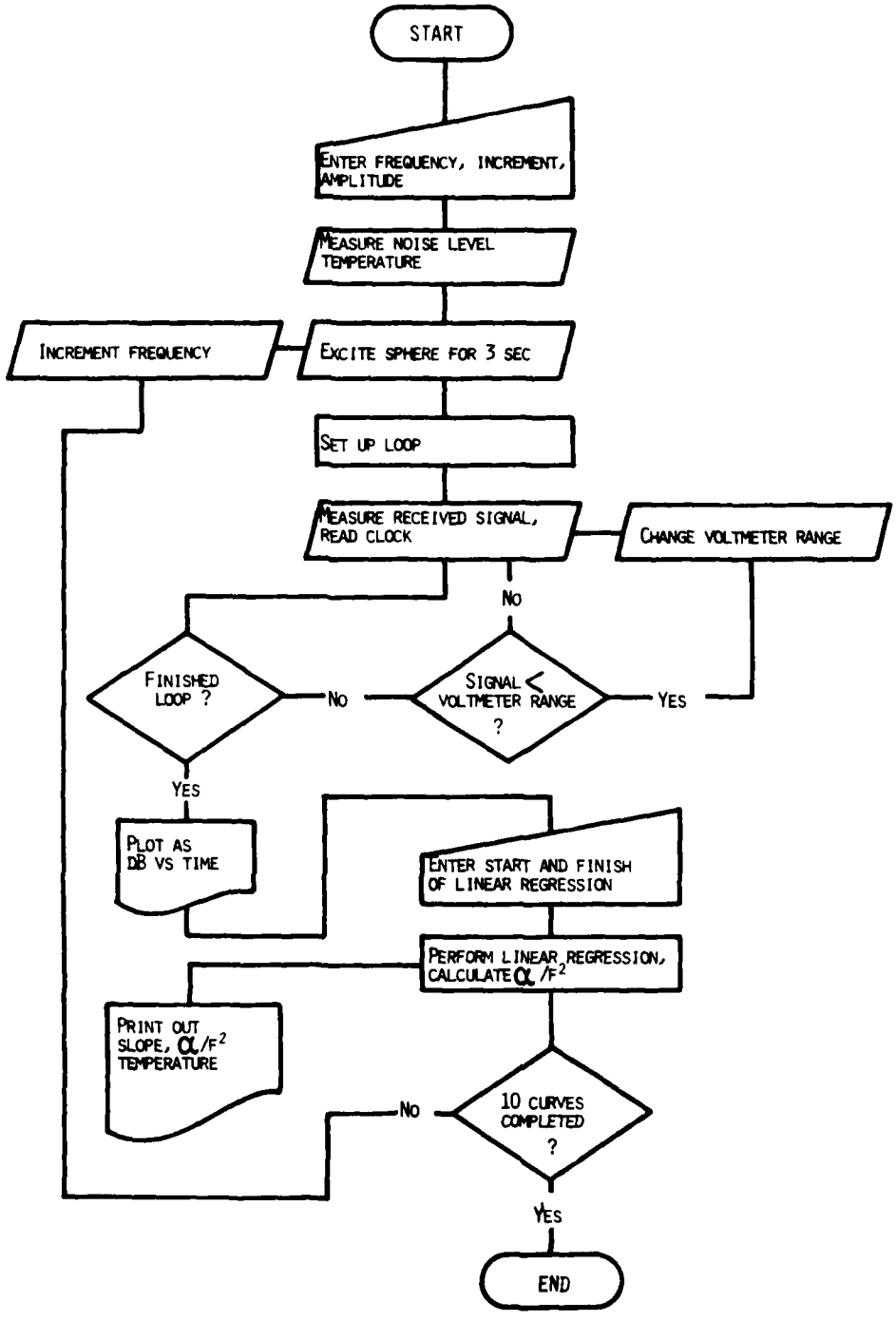

FLOW CHART II

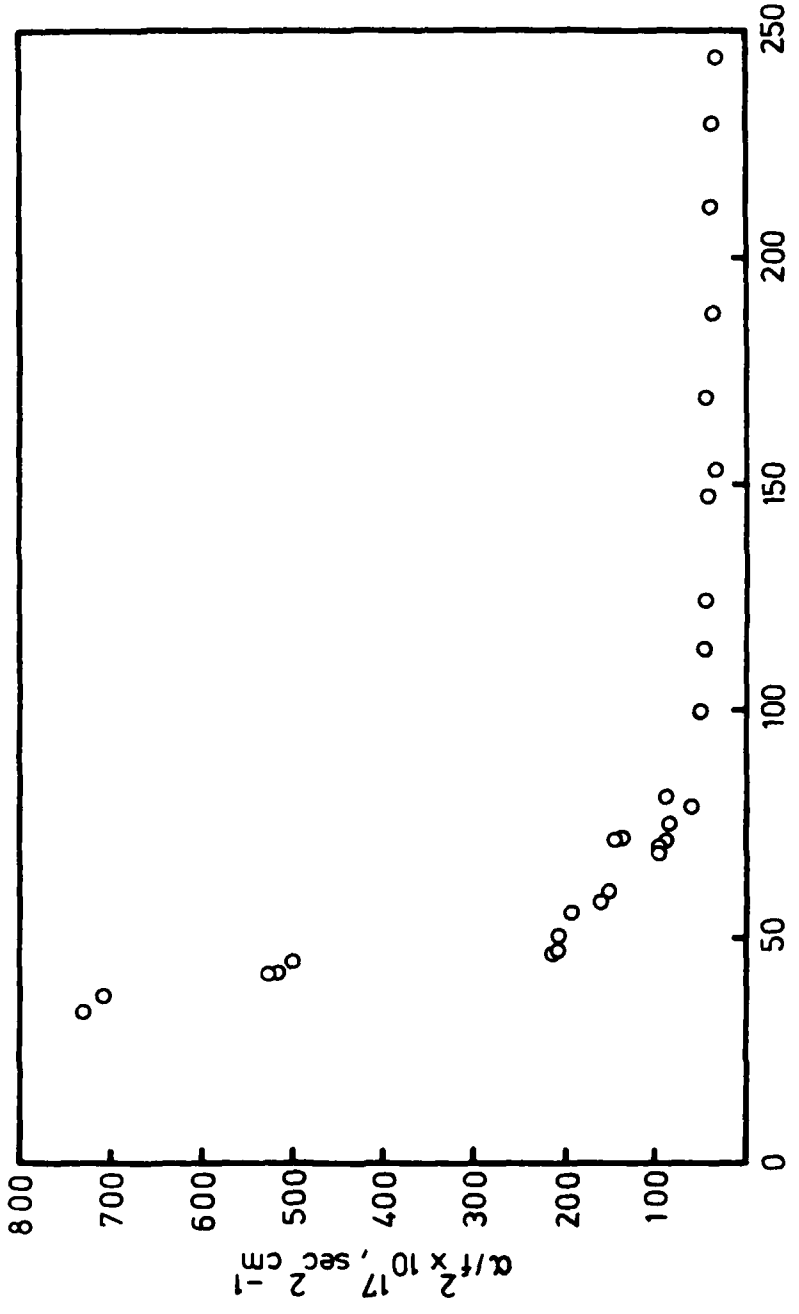

Fig. 11. Plot of the lowest α/f^2 values found with the 12 liter sphere filled with water at 25°C.

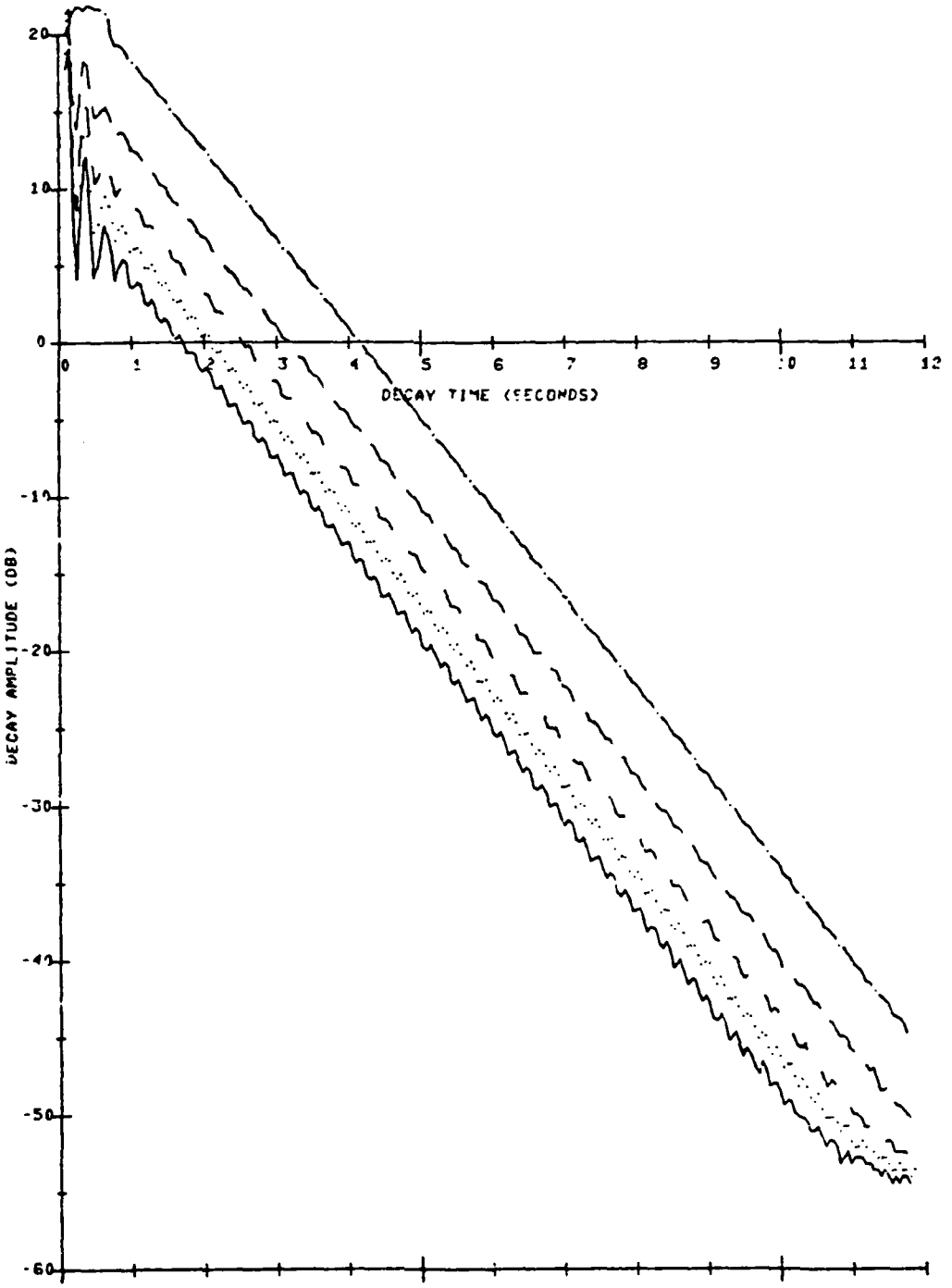

Fig. 12. Sound level versus decay time for frequencies 71401.5 to 71402.3 Hz with increments of 0.2 Hz (see table II). Temperature 25.2°C.

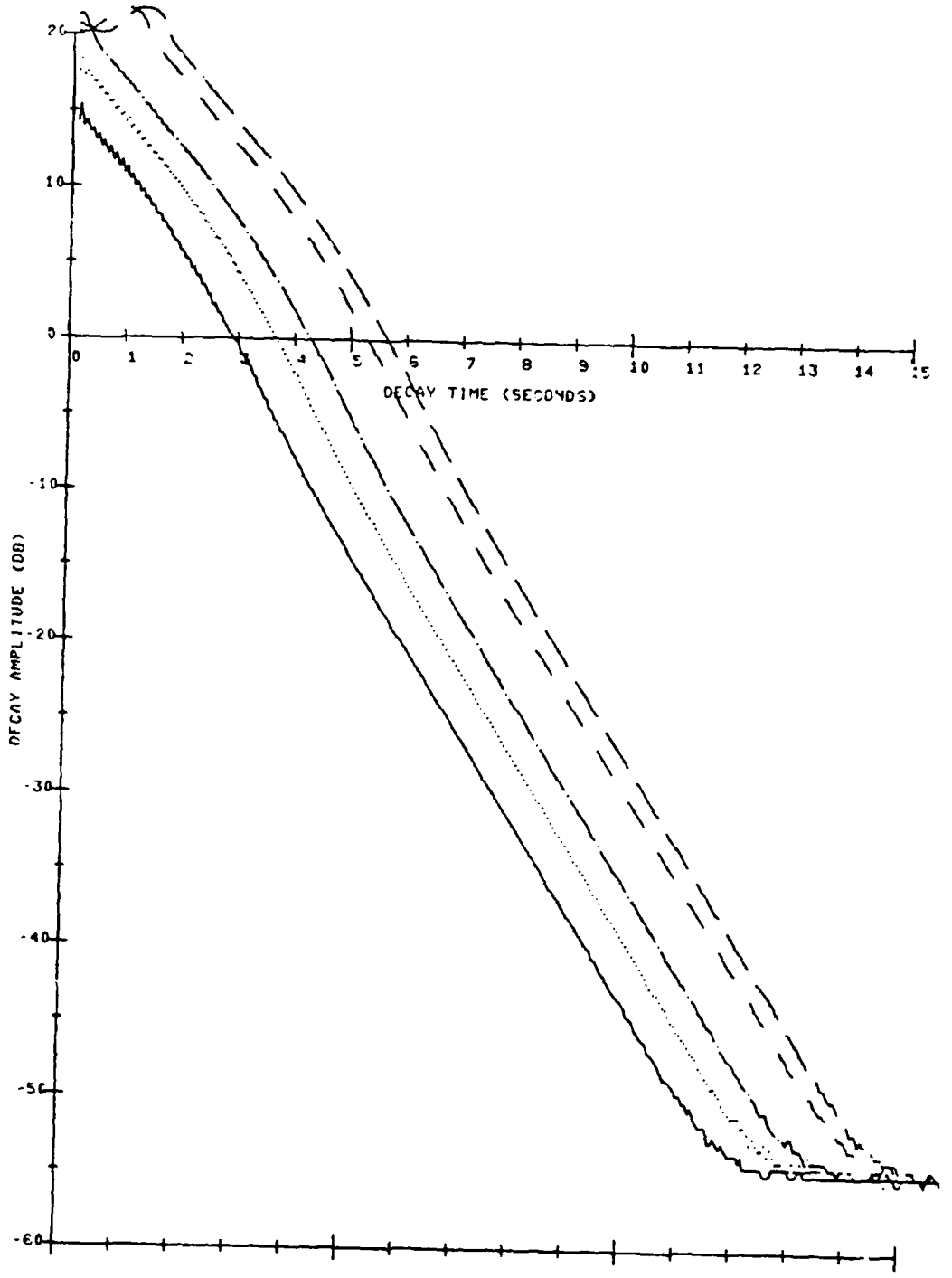

Fig. 13. Sound level versus decay time for frequencies 68824.6 to 68825.5 Hz in increments of 0.3 Hz. Temperature 25.2°C.

ringing, particularly at the beginning of the decay period (see Fig. 12). As the frequency approached the center frequency, this ringing usually died out and a smooth curve was obtained. In this example the values for α/f^2 are given in table II. It can be seen that obtaining the appropriate value for α/f^2 does not depend on finding the precise resonant frequency, as long as a frequency was found sufficiently free of ringing to perform a reasonable linear regression: a few potentially useful peaks were discarded because of excessive slow and persistent ringing.

TABLE II

Constants obtained from the decay curves shown in Fig. 12.

Frequency, Hz	slope, dB/s	$\alpha/f^2 \times 10^{15}$, s^2m^{-1}	correlation coefficient
71401.5	-5.8	88.4	0.99973
71401.7	-5.8	88.4	0.99980
71401.9	-5.8	88.3	0.99989
71402.1	-5.8	88.0	0.99995
71402.3	-5.8	87.8	0.99998

Although most of the peaks given in table I show consistently a straight line over many decades, when deviations from linearity occurred they often altered from day to day. One particular peak is described in more detail as it showed several of the undesirable characteristics that can occur. The most unusual type of behavior is shown in Fig. 13. It is in general expected that when there is more than one mode excited, the faster decaying mode dies out first. The resultant is a concave curve.

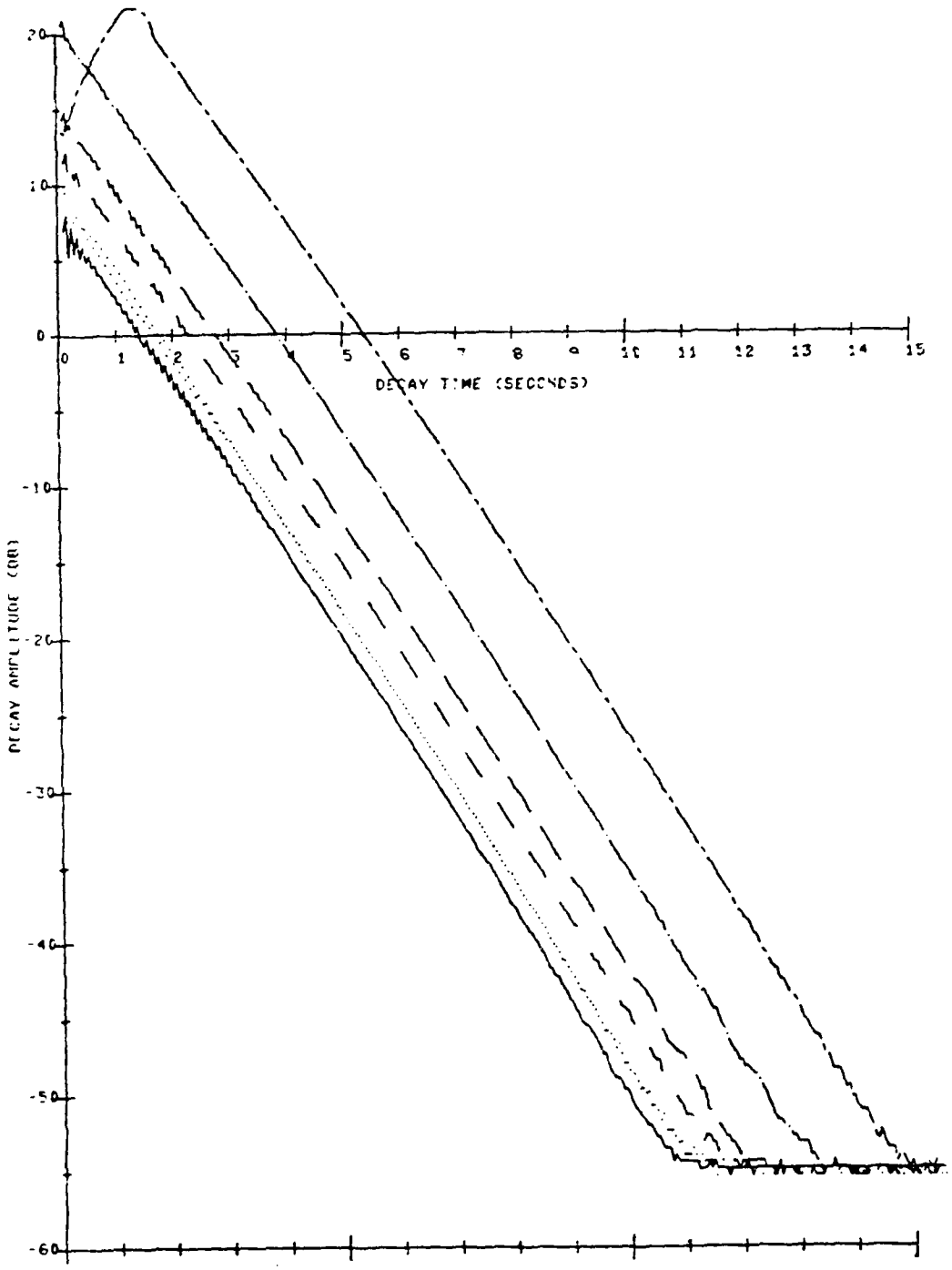

Fig. 14. Sound level versus decay time for frequencies 68823 to 68824.5 Hz in increments of 0.3 Hz, taken on a different day from the data of Fig.13. Temperature 25.2°C.

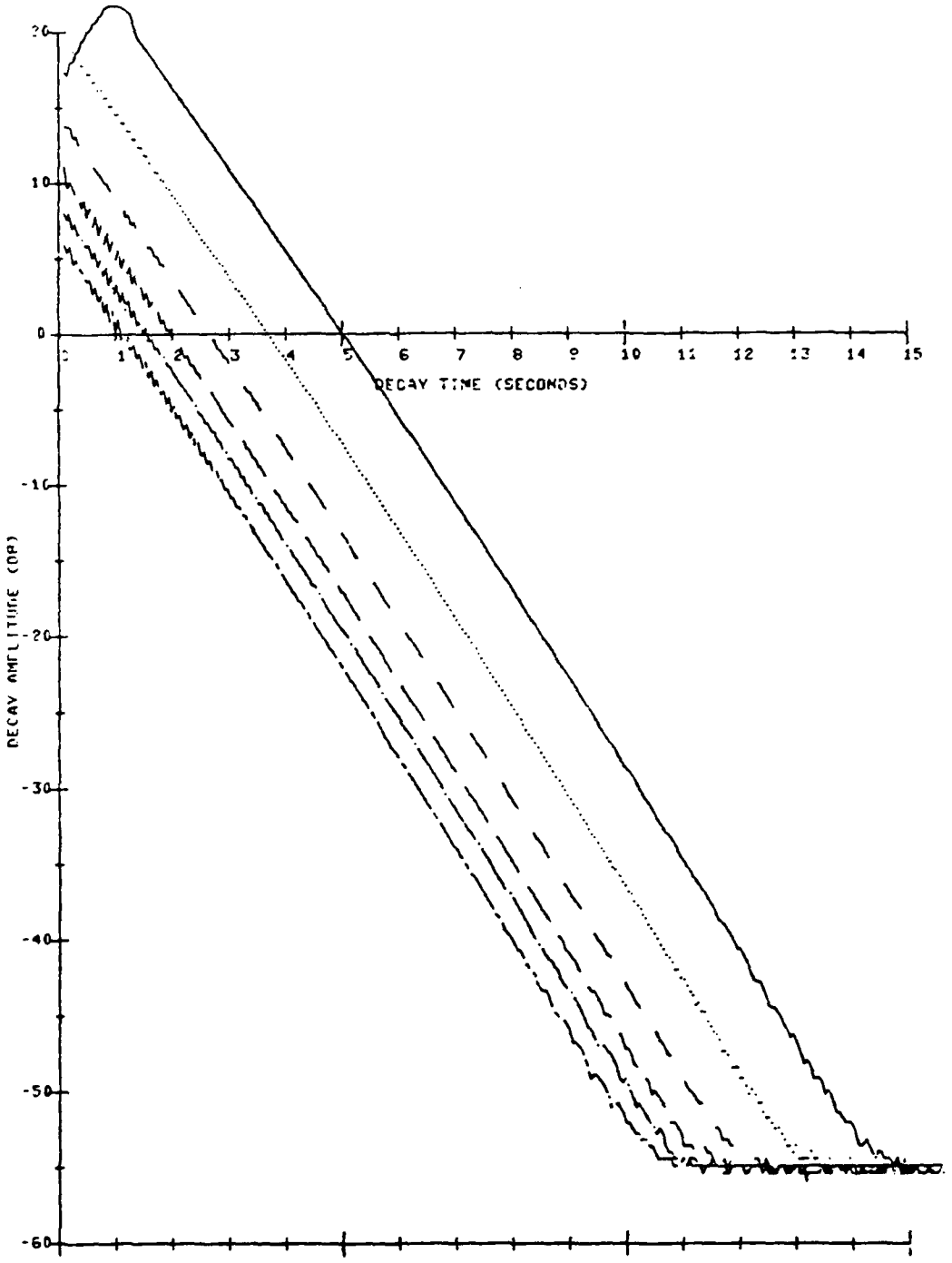

Fig. 15. As Fig. 14 for frequencies68824.5 to 68826 Hz.

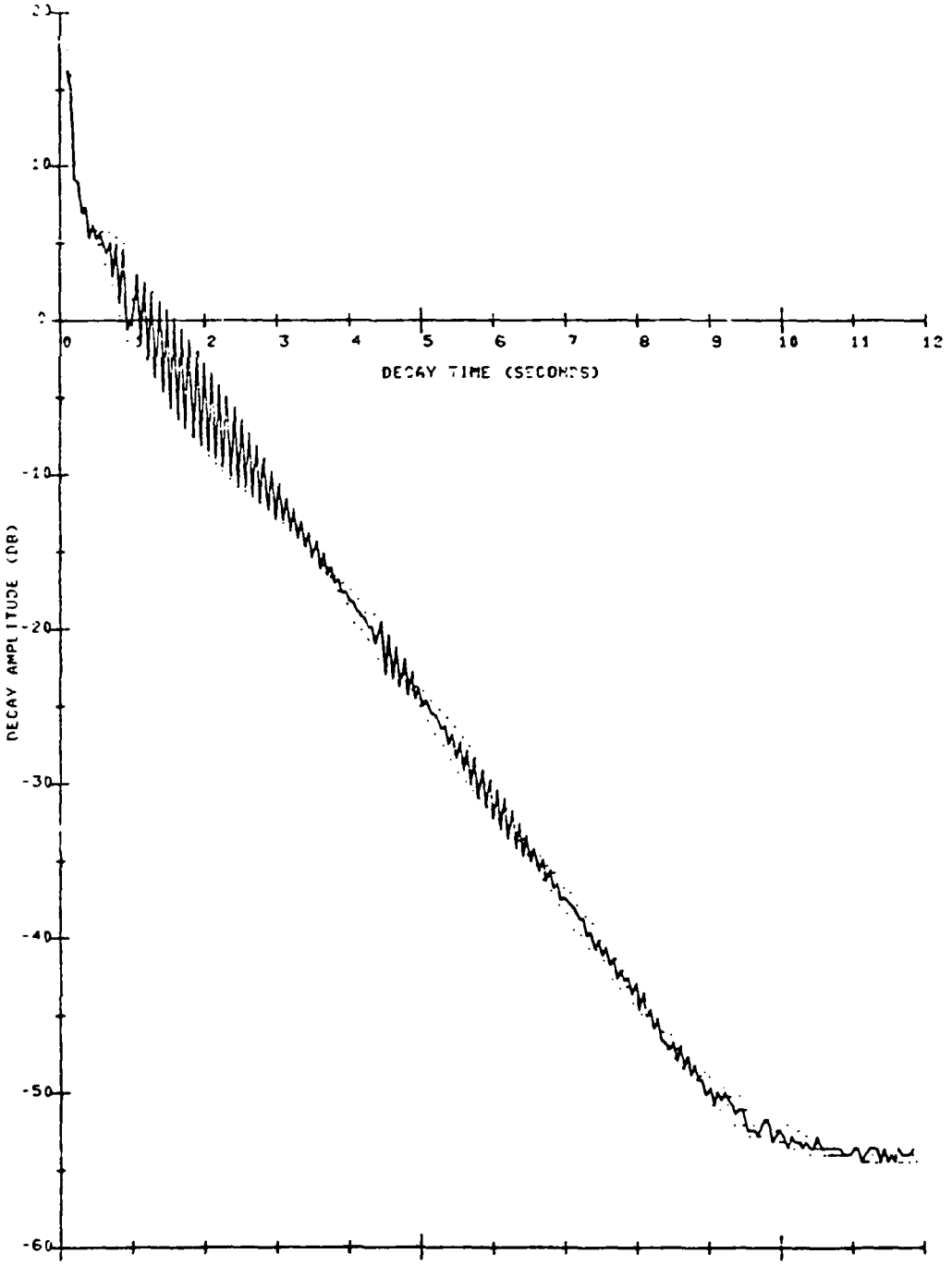

Fig. 16. Sound level versus decay time for frequencies 68861.5 and 68861.8 Hz. Temperature 25.7°C.

The curve in Fig. 13 can better be described as having a lower decay rate initially, with an irregular transition to a higher decay rate. These characteristics disappeared by the time the peak was reinvestigated on another day (Figs. 14 and 15) but a slight smooth convex curvature is still apparent.

After a rise in temperature to 25.7°C, there was a further change in the nature of the curve, Fig. 16. The very small amplitude ringing of 10 Hz frequency just visible in the lower curves of Figs. 14 and 15 mave become more pronounced while the small overall curvature has disappeared. The change in temperature was responsible for the peak shift to 68861 Hz.

D. The use of several transducers

In some early work[1] several transducers have been placed on a 12 liter resonator at various positions with the intent of identifying radial modes, although detailed results were not given. In the case of a spherical shell executing radial oscillations, every point on the shell should oscillate with equal amplitude and in phase. Deviation from this symmetry will result in nodes on the surface. In the present work, some investigations were made with two additional transducers attached at other points on the sphere. In particular, one of the most prominent and slow decaying peaks, 47381 Hz, adopted as a standard for day to day checks, was investigated because this frequency lies directly between two values expected for radial modes (see below). Several observations were made from this study:

1) Mode mapping with the two additional transducers gave the information, for example, that the sphere is not truly oscillating in

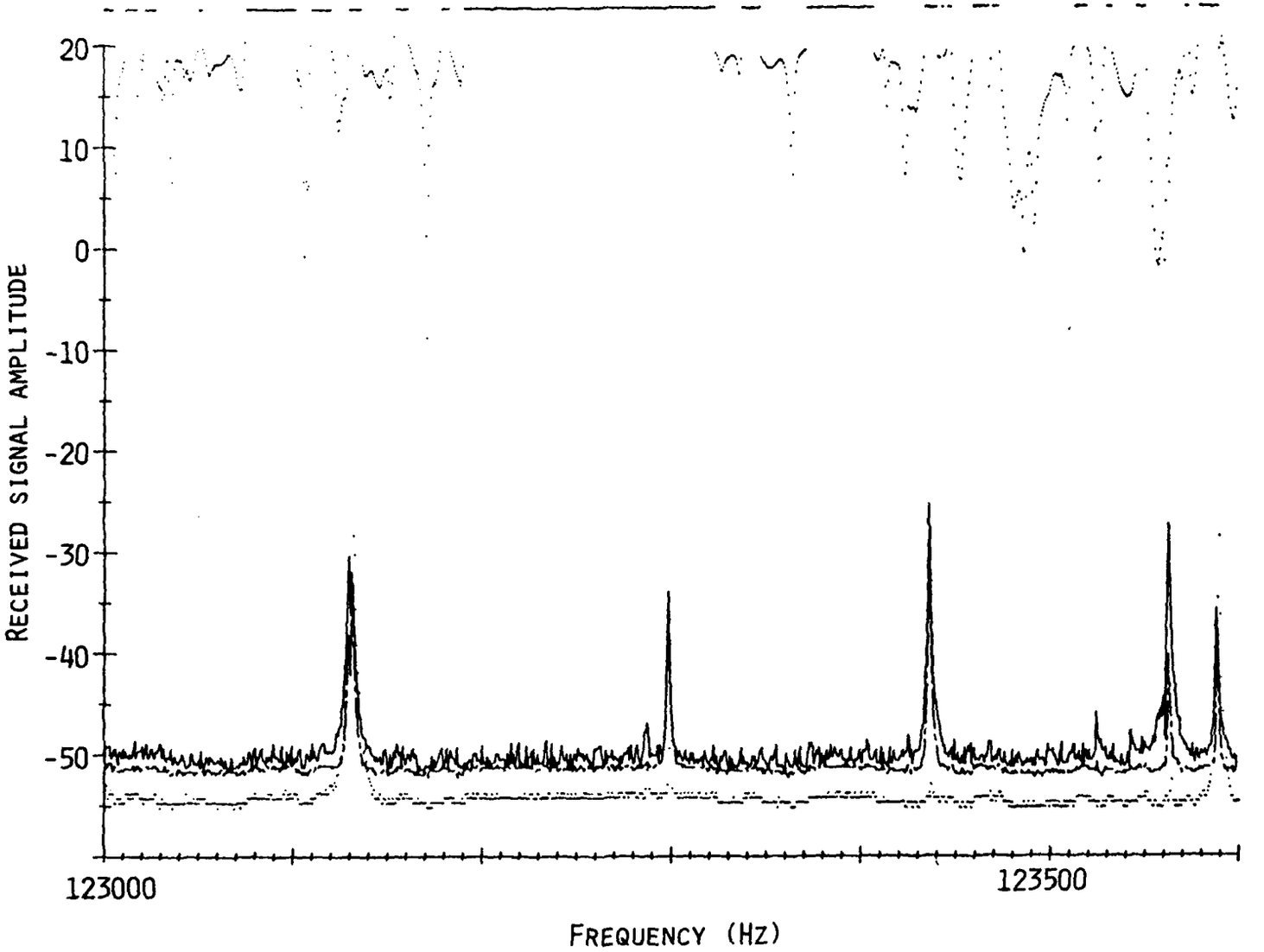

Fig. 17. Mode mapping plot of decay amplitude (dB) versus frequency using three receiving transducers on the 12-liter sphere filled with water. The displace upper two curves represent the signals from the additional transducers.

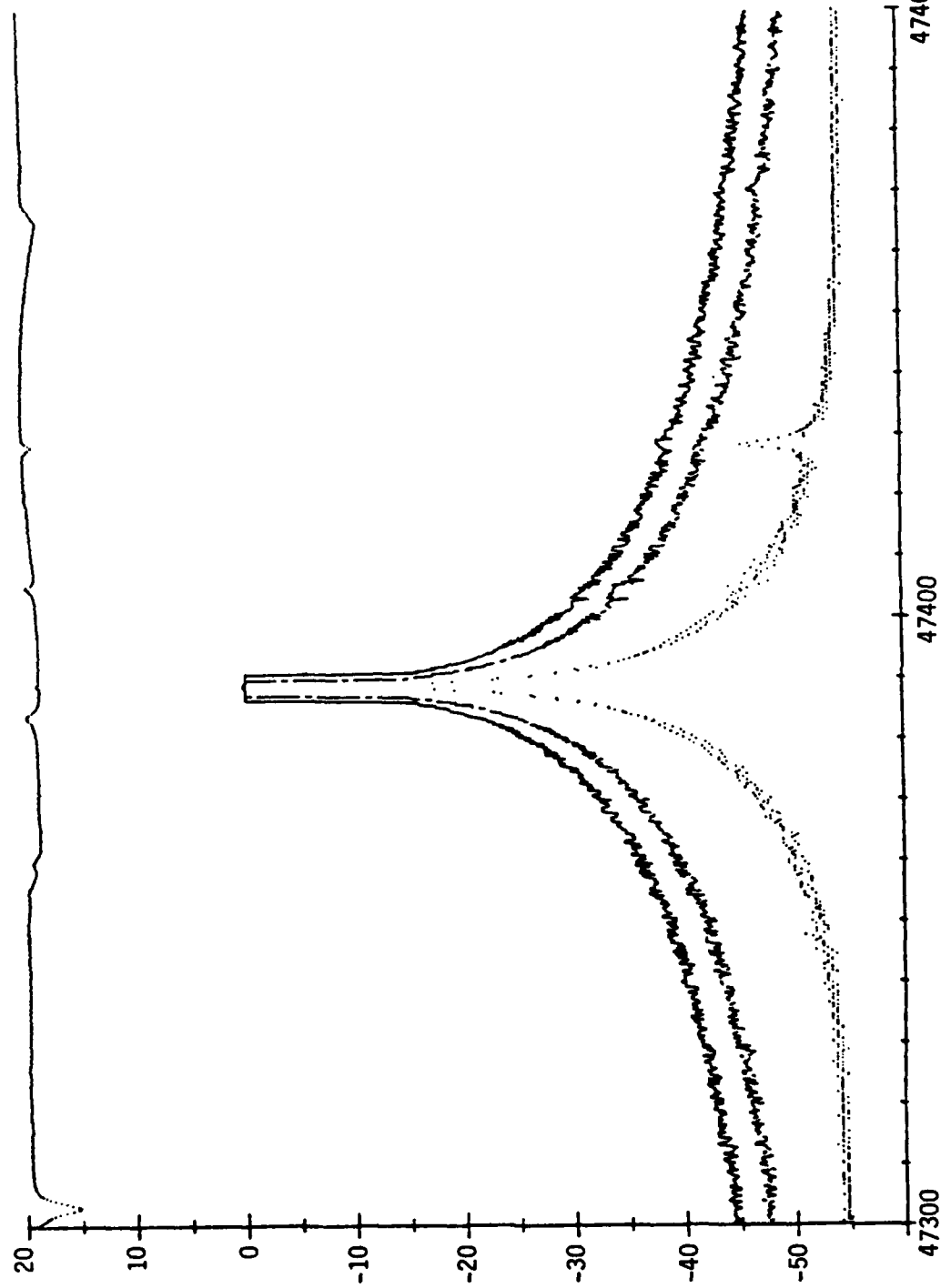

Fig. 18. Mode mapping plot of decay amplitude (dB) versus frequency using three receiving transducers. The displaced upper two curves represent the signals from the additional transducers. Measurements made on the 12-liter sphere filled with water.

the ideal radial mode at frequencies 123300, 123440 and 123570 Hz where only one or two transducers show peaks (see Fig. 17). On the other hand, at 123130, calculated as a radial mode, all transducers respond. At 47380 Hz, although it is not calculated as a radial mode, peaks also appear for all transducers. Fig. 18 shows this peak, and a neighboring peak with much poorer decay rate, which did not show up on the two additional transducer. Decay plots were made with two transducers on the 47381 Hz peak, although decay rates are in general increased by the presence of additional transducers. In this case, the two transducers gave similar decay slopes with rather higher values than usually obtained with a single receiving transducer. It was concluded that this peak on the whole showed the characteristics of a radial mode.

2) Some peaks were shifted on one transducer with respect to another: up to 5 Hz shift was observed. A slight shift is evident from Fig. 17. This could possibly be due to slight deviations of the sphere from the ideal shape, or a slight temperature gradient.

E. Comparison of experiment with calculated radial modes

In earlier work reported in the literature[2], there has been rather poor agreement between the radial mode frequencies to be expected and the slowest decaying modes actually found. The case for the present work is as follows:

Using the measured values of the diameter and wall thickness of the vessel, values of the frequencies were calculated as outlined by Leonard[1] for the radial modes (a summary of Leonards treatment is given in the Appendix). These are shown in table I along with the values of the slowest decaying frequencies found experimentally. Although the α/f^2 values are

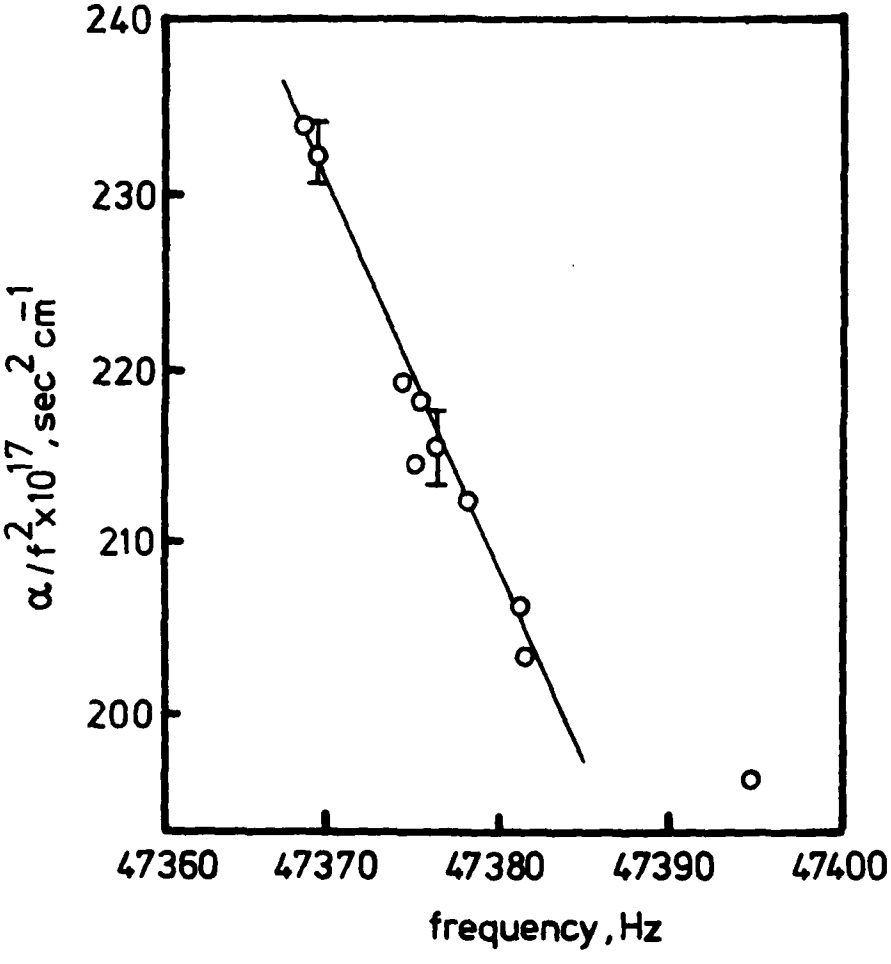

Fig. 19. The variation of α/f^2 values for the peak around 47381 Hz over a 14 day period plotted against peak frequency. Temperature fluctuations caused the peak frequency to shift.

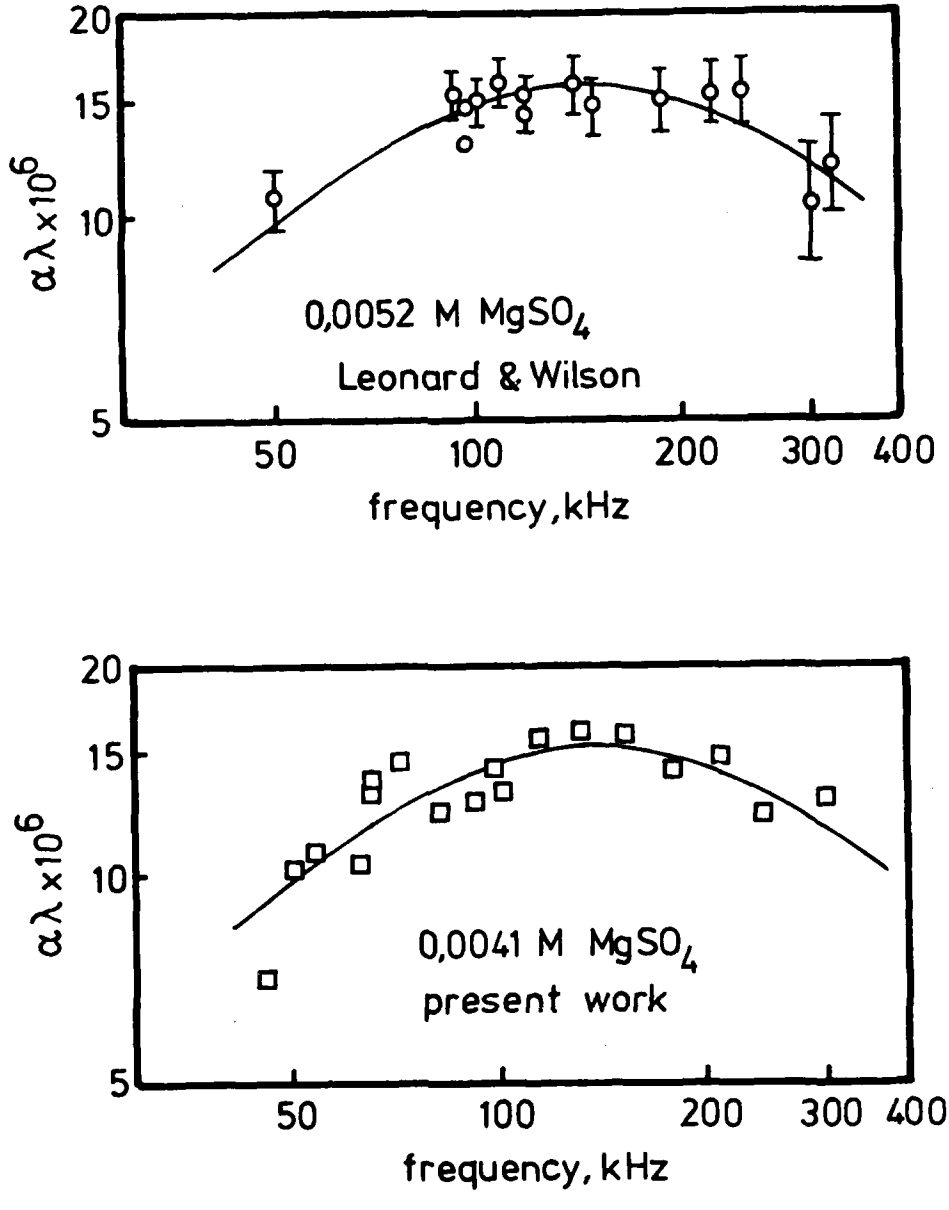

Fig. 20 Comparison between the relaxation absorption of $MgSO_4$ solution obtained with manual and computer controlled experiments.

poorer that those of Wilson[2], the experimentally found frequencies are in closer agreement with the theoretical values. It is noteworthy that a number of the slowest decaying modes occur at frequencies almost directly between two predicted modes.

The deviations from expected values cannot be explained by temperature fluctuations, which never exceeded $\pm 0.5^{o}C$. In a 14 day investigation of the particular frequency 47381 Hz, it was found that variations of temperature in the vessel caused variations in the peak frequency of .048%. This corresponds to a temperature shift of $0.26^{o}C$. A clear correlation between the α/f^2 values and the peak frequency was found, as seen in Fig. 19. The change in α/f^2 is too large to be explained by the change of acoustic absorption of water with temperature, and is more likely indicating a change in wall losses or temperature gradients. This behavior was not necessarily followed by other peaks or at other times.

At different temperatures, different peaks become dominant. A similar situation is also evident from Wilson's work at various temperatures[2] where different peaks are listed in the tables for the various temperatures.

F. Relaxation curve for $MgSO_4$ solution

As a means of testing the present setup for determining excess absorption on a system, a solution of 0.0041M $MgSO_4$ was introduced into the 12-liter sphere.

For comparison, our results are shown on the same page as those of Wilson[2] (Fig. 20 a and b) at the most nearly corresponding concentration (0.0053 M) and temperature ($24^{o}C$). The relaxation frequency derived from our results agrees with theirs, and also with both Stuehr[8] and Wilson for a concentration of 0.01 M. Concentration dependence of relaxation frequency

is indeed not expected. However, it must be pointed out that Wilson's results for several other concentrations show a higher relaxation frequency, and the results overall would suggest a slight concentration dependence.

The previous investigators have mentioned the particular difficulty in obtaining reliable results at the low frequencies. This is born out by the fact that Wilson gives only one point under 100 kHz in their curve for 0.0053 M $MgSO_4$. It was noted above in a discussion of the 47381 Hz resonance peak that the attenuation value varied with temperature much more than expected from the known dependence of α on temperature for water. At these low frequencies, a large proportion of the observed attenuation is due to wall losses, and variations in these are poorly understood. We have found eight resonance peaks which are usable below 100 kHz at this concentration. However, in several cases where clusters of peaks occur, the slowest decay rate will not necessarily be the exact same member of the cluster for both water and $MgSO_4$. Below 47 kHz, no reasonable data could be obtained for the excess absorption due to $MgSO_4$; clearly the larger resonance sphere must be used for this range, since wall losses are much reduced.

Comparison of the 12-liter and the 100-liter sphere.

The 100-liter sphere shows a remarkable decrease in wall losses at low frequencies compared to the 12-liter plass sphere. For example, the peak at 22.7 kHz with the 100-liter sphere, shown in Fig. 10, gave a value for α/f^2 of 100.5 x $10^{-15} s^2 m^{-1}$. By comparison, water in the 12-liter sphere gave α/f^2 = 2096 x $10^{-15} s^2 m^{-1}$ at the frequency 22.5 kHz. These were respectively the lowest decaying modes in that frequency range. If the true value of α/f^2 for water is 22 x $10^{-15} s^2 m^{-1}$, and the remainder of the

observed attenuation is due to wall losses, these figures indicate that the wall losses contribution of the titanium sphere is only 4% of that of the 12-liter sphere.

The resonance peak of 22.7 kHz, with a decay rate of 0.68 dB/s indicates a Q value of 8.9×10^5. This is comparable to the value reported by Fisher[9] .

Conclusions

The computer controlled spherical resonator allows a very much more thorough search of all the resonance modes for a reasonable effort than manually controlled apparatus, as well as more accurate an convenient determination of decay rates.

The results on the whole agree well with those obtained by earlier workers. The agreement between theoretical and experimental frequencies for radial mode resonances, although closer than found in earlier work, still contains some discrepancies, and these are not understood. A limited investigation with several transducers attached to the sphere was not able to resolve the matter. As is the usual practice, the lowest decay rates are considered to give the appropriate attenuation values for use in comparison of varous samples. On this basis, it was possible, by comparison of the measurements in water and $MgS)_4$ solution, to derive reasonable values for the excess absorption of $MgSO_4$, and obtain a relaxation curve with a larger number of useful points at the lower part of the frequency range than previously attained under similar conditions. However, useful results for this type of comparison can only be obtained above 47 kHz with the 12-liter sphere. Since difficulties are largely associated with

wall losses, which are poorly understood, much improvement can be expected by the use of the 100-liter sphere. The improvement with this sphere is illustrated by the fact that the wall losses at 22 kHz are reduced to 4% of that found with the 12-liter sphere.

REFERENCES

1. R.W. Leonard, "The Attenuation of Sound in Liquids by a Resonator Method", Technical report No. 1, June (1950), Office of Naval Research, Contract N7, ONR-27507, Project Nr 014-302.
2. O.B. Wilson Jr., "Absorption of Ultrasonic Waves in Aqueous Solution of Magnesium Sulphate", Technical report No.4, June 1951, Office of Naval Research, Contract N6, ONR-27507, Project Nr 014-302.
3. R.H. Mellen, V.P. Simmons and D.G. Browning, J. Acoust. Soc. Am. 65, 923 (1979).
4. J.B. Mehl and M.R. Moldover,J. Acoust. Soc. Am. Suppl. 1 S19, 67, (1980).
5. R.J. Lambert, J. Acoust. Soc. Am., 25, 1068 (1953).
6. A.L. Anderson and L.D. Hampton, J. Acoust. Soc. Am., 67, 1891, (1980).
7. A. Labhardt and G. Schwarz, Berichte der Bunsen-Gesellschaft, Bd 80, Nr 1 p.83 (1976).
8. J.E Stuehr, "Ultrasonic Relaxation Processes in Electrolytic Solutions" Ph.D. Thesis, Dept. of Chemistry, Western Reserve University (1961) Cleveland, Ohio.
9. C.C. Hsu and F.H. Fisher, J. Acoust. Soc. Am. Suppl. 1 69, S44 (1981).

Appendix

The neck opening of the spherical vessel used in this study was very small compared to the circumference of the sphere. We can make the assumption that the spherical surface is nearly complete and the flexural oscillations must approximate to those of a complete sphere. It is also assumed that when the wall thickness of the vessel is small, the tangetial component of displacement of the spherical shell is small compared to the normal component(radial component).

Leonard[1] gave an approximate method for calculation of the effect of a finite but small boundary thickness on the decay rate of a resonator due to the wave propagation in this boundary.

After making the following assumptions and assuming wave numbers k_1 and k_2 are real, and taking into account 0th and first order approximations for k_1 and k_2

$$k_1 = (\omega/c_1) + i\,\alpha_1$$

$$k_2 = (\omega/c_2) + i\,\alpha_2$$

where $\omega = 2\,\pi_o f$, f is the frequency and α is the attenuation coefficient and c is the velocity of sound, where subscripts 1 and 2 designate fluid medium and resonator wall respectively.

The predicted radial mode frequencies f_m, can be calculated by

$$f_m = \frac{k'_{1m} c_1}{2\pi}$$

where $k'_{1m} = \dfrac{m\pi + \varepsilon}{R_1}$

and $\tan \varepsilon = \dfrac{m\pi}{1 - \dfrac{\rho_1}{\rho_2} - \dfrac{\rho_1}{\rho_2}\, R_1\, k^o_{2m}\, \mathrm{Ctn}\left\{k^o_{2m}\, d\right\}}$

where overscript 0 and 1 refer to 0th and 1st order approximations of k_{1m} or k_{2m} and m is the integer, R is the radius of the sphere and ρ is the density of the medium, d is the thickness of the spherical shell (resonator).

REPORTS DISTRIBUTION LIST FOR ONR PHYSICS PROGRAM OFFICE
UNCLASSIFIED CONTRACTS

Director Defense Advanced Research Projects Agency Attn: Technical Library 1400 Wilson Blvd. Arlington, Virginia 22209	3 copies
Office of Naval Research Physics Program Office (Code 421) 800 North Quincy Street Arlington, Virginia 22217	3 copies
Office of Naval Research Director, Technology (Code 200) 800 North Quincy Street Arlington, Virginia 22217	1 copy
Naval Research Laboratory Department of the Navy Attn: Technical Library Washington, DC 20375	3 copies
Office of the Director of Defense Research and Engineering Information Office Library Branch The Pentagon Washington, DC 20301	3 copies
U. S. Army Research Office Box 12211 Research Triangle Park North Carolina 27709	2 copies
Defense Technical Information Center Cameron Station Alexandria, Virginia 22314	12 copies
Director, National Bureau of Standards Attn: Technical Library Washington, DC 20234	1 copy
Commanding Officer Office of Naval Research Western Regional Office 1030 East Green Street Pasadena, California 91101	3 copies
Commanding Officer Office of Naval Research Eastern/Central Regional Office 666 Summer Street Boston, Massachusetts 02210	3 copies

Director
U. S. Army Engineering Research
and Development Laboratories
Attn: Technical Documents Center
Fort Belvoir, Virginia 22060 — 1 copy

ODDR&E Advisory Group on Electron Devices
201 Varick Street
New York, New York 10014 — 3 copies

Air Force Office of Scientific Research
Department of the Air Force
Bolling AFB, D. C. 22209 — 1 copy

Air Force Weapons Laboratory
Technical Library
Kirtland Air Force Base
Albuquerque, New Mexico 87117 — 1 copy

Air Force Avionics Laboratory
Air Force Systems Command
Technical Library
Wright-Patterson Air Force Base
Dayton, Ohio 45433 — 1 copy

Lawrence Livermore Laboratory
Attn: Dr. W. F. Krupke
University of California
P.O. Box 808
Livermore, CAlifornia 94550 — 1 copy

Harry Diamond Laboratories
Technical Library
2800 Powder Mill Road
Adelphi, Maryland 20783 — 1 copy

Naval Air Development Center
Attn: Technical Library
Johnsville
Warminster, Pennsylvania 18974 — 1 copy

Naval Weapons Center
Technical Library (Code 753)
China Lake, California 93555 — 1 copy

Naval Training Equipment Center
Technical Library
Orlando, Florida 32813 — 1 copy

Naval Underwater Systems Center
Technical Center
New London, Connecticut 06320 — 1 copy

Commandant of the Marine Corps — 1 copy
Scientific Advisor (Code RD-1)
Washington, DC 20380

Naval Ordnance Station — 1 copy
Technical Library
Indian Head, Maryland 20640

Naval Postgraduate School — 1 copy
Technical Library (Code 0212)
Monterey, California 93940

Naval Missile Center — 1 copy
Technical Library (Code 5632.2)
Point Mugu, California 93010

Naval Ordnance Station — 1 copy
Technical Library
Louisville, Kentucky 40214

Commanding Officer — 1 copy
Naval Ocean Research & Development Activity
Technical Library
NSTL Station, Mississippi 39529

Naval Explosive Ordnance Disposal Facility — 1 copy
Technical Library
Indian Head, Maryland 20640

Naval Ocean Systems Center — 1 copy
Technical Library
San Diego, California 92152

Naval Surface Weapons Center — 1 copy
Technical Library
Silver Spring, Maryland 20910

Naval Ship Research and Development Center — 1 copy
Central Library (Code L42 and L43)
Bethesda, Maryland 20084

Naval Avionics Facility — 1 copy
Technical Library
Indianapolis, Indiana 46218


DA
FILM